ISSN: 1224-7626

ANALELE UNIVERSITĂŢII DIN ORADEA

Fascicula CHIMIE
XXVIII (28)

EDITURA UNIVERSITĂŢII DIN ORADEA

2021

Editor in chief: BADEA Gabriela Elena
gbadea@uoradea.ro

Editors
Gultekin Tarcan – Dokuz Eylul University, Turkey, gultekin.tarcan@deu.edu.tr
Cavit Uyanik - Kocaeli University, Kocaeli, Turkey, cuyanik@kocaeli.edu.tr
Hrefna Kristmannsdottir-Efla Engineering Company, Iceland
Jantschi Lorentz- Technical University of Cluj Napoca, România,lorentz.jantschi@gmail.com
Ioniţă Daniela- University Politehnica of Bucharest, România, md_ionita@yahoo.com
Cojocaru Anca- University Politehnica of Bucharest, România, a_cojocaru@chim.upb.ro
Maior Ioana- University Politehnica of Bucharest, România, i_maior@chim.upb.ro
Dumitrescu Vasile - Universitatea Petrol-Gaze din Ploiesti
Iovi Aurel - University Politehnica Timişoara, România
Gilău Ludovic – University of Oradea, România
Bungău Simona – University of Oradea, România, simonabungau@gmail.com
Badea Gabriela Elena- University of Oradea, România, gbadea@uoradea.ro
Fodor Alexandrina - University of Oradea, România, afodor@uoradea.ro
Cărăban Alina - University of Oradea, România, acaraban@uoradea.ro
Stănăşel Oana - University of Oradea, România, ostanasel@uoradea.ro
Gavriş Georgeta- University of Oradea, România, georgeta_gavris@uoradea.ro
Hodişan Sorin - University of Oradea, România, sorin.hodisan@yahoo.com
Sebeşan Mioara - University of Oradea, România, msebesan@uoradea.ro
Cozma Alina - University of Oradea, România, acozma@uoradea.ro
Bota Sanda - University of Oradea, România, sbota@yahoo.com
Petrehele Anda - University of Oradea, România, pcorinamara@yahoo.com
Morgovan Claudia - University of Oradea, România, cmorgovan@yahoo.com

Editorial Adress
University of Oradea, Chemistry Departament
Str. Universitatii, nr.1, 410087, Oradea, Bihor, România
General Information
ISSN: 1224-7626
Place of publishing: Oradea, Romania
Year of the first issue: 1995
Releasing frequency: 1 issue / year
Language: English
Abstracting/Indexing:

Chemical Abstracts Service-CAS Source Index (CASSI)

Academic Research Index- ResearchBiB

TABLE OF CONTENTS

Analele Universităţii din Oradea-Fascicula Chimie, Vol. XXVIII(28), 2021

Zn II, Cu II, Pb II, Hg II, Ni II SURVEY AND THE SURFACE WATERS QUALITY EVALUATION IN THE BARCĂU RIVER BASIN (WEST ROMANIA)

Sorin HODIŞAN [1], Alexandrina FODOR [1], Sanda BOTA [1],
Mioara SEBEŞAN [1]

[1]University of Oradea, Faculty of Informatics and Sciences, 1 University St.,
410048,Oradea, Romania, e-mail: afodor@uoradea.ro

Abstract-*The survey of Zn, Cu, Pb, Hg and Ni ions in the surface waters of Barcau River Basin (West Romania), the evaluation of their quality in order to classify them by water quality classes point of view and the analyse of the influence of anthropogenic factors have been made. The water samples were taken from six sampling points, during February-November 2018. Metal ions concentration were measured using atomic absorption method. The smallest quantities of metal ions were registered, as expected, in Tusa, in the upper part of the River Barcău. An increase of metal ions concentrations in the summer months was registered. Smaller metal ions quantities were measure also downstream of Pădurea Neagră City than in the case of the other investigated localities. In Tusa and Padurea Neagră sampling points the surface water can be classified in class I of quality regarding all metallic ions investigated. In Boghiş and Suplacul de Barcău sampling points the surface water was classified in class II and III of quality regarding some of the metallic ions investigated. At the border with Hungary (Parhida) the water of the Barcău River falls in the quality class I in terms of the content of Pb II and Hg II and in the quality class II in terms of the content of Zn II, Cu II and Ni II. In order to prevent pollution of the Barcău River Basin, it is necessary to take measures to remove the wastewater discharge without prior treatment.*

Key words: survey, surface water quality, dissolved fraction metal

INTRODUCTION

The evaluation and the survey of surface water quality is based on the determination of its physical, chemical, biological and microbiological properties (Jude, 2014). The information obtained from the monitoring of surface waters allows the achievement of four primary objectives in knowing the state of water quality such as monitoring, forecasting, warning and intervention (Domuţa et al. 2011). By monitoring the water quality, a systematic evaluation of the qualitative characteristics of the water is performed, which are in a permanent dynamic and with significant socio-economic implications (Cîrţînă, 2011).

Heavy metals are elements that have a high atomic weight and a density (five times greater than that of water). Their multiple industrial, domestic, agricultural, medical, and technological applications have led to their wide distribution in the environment (especially in soil and water). Their continuously raise concentrations in the environment produce serios concerns over their potential effects on human health and the environment. Their toxicity depends on several factors including the dose, route of exposure, and chemical species, as well as the age, gender, genetics, and nutritional status of exposed individuals. These metallic elements are considered systemic toxicants that are known to induce multiple organ damage, even at lower levels of exposure(Tchounwou et al. 2012).

They are also classified as human carcinogens (known or probable) according to the US Environmental Protection Agency (https://www.epa.gov/) and the International Agency for Research on Cancer (https://www.iarc.who.int/).

Recording the data obtained by the monitoring of surface water quality, an assessment is made in order to evaluate if the water quality meets the current regulatory requirements, water quality being influenced by both natural and anthropogenic factors generated by urbanization and industrialization, surface water being an important factor of the environment (being the support of ecological systems) but also an important staple material (Gavriș, 2003; Varduca, A. 2000).

The Barcău River Basin is a component of the Crişuri Rivers Basin system. The source point of the Barcău River is at the foot of the plateau of the Șes Mountains (altitude 585 m), Tusa Village, Sălaj County. The length of the course is 134 km and the surface of the reception basin and of the tributaries is of the order of 2005 km^2 (http://arhiva.rowater.ro/dacrisuri). The river has a length of 134 km on the Romanian territory, an average slope of 4 ‰ and a sinuosity coefficient of 1.72, and the surface of the collecting basin is 2005 km^2. It collects 28 tributaries, of which the most important are Bistra (L = 47 km, S = 175 km^2), Valea Fâneţelor / Ghepeș (L =30 km, S=178 km^2). (http://www.mmediu.ro;http://chislaz.ro/).

In the Barcău River Basin, the main polluting units are: urban activities, extractive industry units (eg OMV Petrom Suplacul de Barcău), food industry units, electricity and heat generating units, trade and services units for the population, tourist thermal units (for example Boghiş Baths).

The assay of theirs study was the survey of divalent ions of Zn, Cu, Pb, Hg and Ni content in the dissolved fraction in the Barcău River Basin during February-November 2018, in six sampling points. The sampling points were located on two important tributaries of the Barcau: on the Rachitelor Valley and Bistra and on Barcău River, downstream of the localities: Tusa (at the spring), Boghiş, Pădurea Neagră, Suplacul de Barcău, Marghita, and Parhida (before crossing the border with Hungary).

MATERIAL AND METHOD

Water sampling and investigations were performed according to the literature information (Pătroescu et al. 2000; Eaton and Franson, 2005).

The water samples were taken in 100-150 mL polyethylene containers. To preserve the water samples, the water was filtered immediately after the sampling, on a membrane filter with 0.45 µm pore diameter and acidified with nitric acid at pH 1-2.

The metal ions analysis was performed by atomic absorption spectrophotometry, comparing the absorption of the sample with the absorbances of the standard solutions. (SREN ISO15586, 2004)

An EM 16.0 atomic absorption spectrometer with cathode lamps corresponding to the analysed metals it was used. The reagents used were concentrated nitric acid, hydrochloric acid, acetate buffer, 1,10-phenanthroline, standards for the construction of the standard curve, purchased from Merck.

RESULTS AND DISCUSSION

During February-November 2018, water samples were taken from the established areas with the frequency of one sample per week. The results obtained following the atomic absorption analysis of the divalent ions of Zn, Cu, Pb, Hg and Ni in the sampled surface water are presented as monthly arithmetic average in tables no. 1-5.

Table. 1 Zn (II) concentration (µg / L) in the surface water samples

Sampling point/ Month	Tusa	Pădurea Neagră	Boghiș	Suplacu de Barcău	Marghita	Parhida
February	4.10	7.12	21.12	25.40	19.42	18,60
March	4.92	7.74	25.34	27.40	22.60	19,40
June	5.34	7.30	26.30	28.42	23.32	19,92
Julie	5.62	8.32	26.72	28.64	24.54	21,34
October	5.30	8.70	27.90	28.90	23.72	22,32
November	4.80	7.50	24.92	26.72	22.10	20,14

Table 2. Cu(II) concentration (µg / L) in the surface water samples

Sampling point/ Month	Tusa	Pădurea Neagră	Boghiș	Suplacu de Barcău	Marghita	Parhida
February	1.10	1.60	4.22	8.20	5.42	5.30
March	1.30	1.70	4.42	8.60	5.80	5.52
June	1.42	1.90	4.52	8.70	5.90	5.60
Julie	1.32	1.82	4.50	8.82	6.22	5.84
October	1.64	1.64	4.74	8.60	5.80	5.70
November	1.20	1.40	4.32	8.40	5.70	5.52

Table 3. Pb(II) concentration (µg / L) in the surface water samples

Sampling point/ Month	Tusa	Pădurea Neagră	Boghiș	Suplacu de Barcău	Marghita	Parhida
February	0.42	0.50	0.80	2.02	0.92	0.80
March	0.40	0.60	0.70	2.10	1.20	0.70
June	0.64	0.70	0.62	1.94	0.84	0.92
Julie	0.42	0.82	0.92	2.24	0.92	0.80
October	0.32	0.64	0.74	2.10	0.90	0.72
November	0.20	0.50	0.50	2.30	0.80	0.84

Table 4. Hg (II) concentration (µg / L) in the surface water samples

Sampling point/ Month	Tusa	Pădurea Neagră	Boghiș	Suplacu de Barcău	Marghita	Parhida
February	0,01	0,04	0,08	0,07	0,06	0,04
March	0,04	0,03	0,07	0,06	0,05	0,05
June	0,05	0,04	0,06	0,09	0,08	0,05
Julie	0,06	0,06	0,08	0,08	0,07	0,06
October	0,07	0,02	0,07	0,07	0,04	0,04
November	0,06	0,03	0,05	0,05	0,05	0,04

Table 5. Ni (II) concentration (µg / L) in the surface water samples

Sampling point/ Month	Tusa	Pădurea Neagră	Boghiș	Suplacu de Barcău	Marghita	Parhida
February	1,2	1,5	3,8	4,2	3,6	3,7
March	1,3	1,7	3,9	4,4	3,4	3,9
June	1,2	1,9	4,1	4,6	3,8	4,2
Julie	1,4	1,6	4,2	4,7	4,0	3,9
October	1,6	1,7	3,9	4,4	3,9	3,8
November	1,4	1,5	3,6	4,5	3,5	3,6

The obtained results show higher concentrations of metallic ions in the surface water samples in March-July period, in all samples points.

As expected, the lowest values of the concentrations for the determined species were recorded in Tusa (at the source of the River). Low values were also recorded downstream of Pădurea Neagră.

RESULTS INTERPRETATION

Analysing the obtained experimental data, from the six sampling points, with the concentration limits imposed by the norm for the classification of surface waters (table no. 6), the analysed waters were classified in classes I, II and III of quality (table no.7) according to ion content of the dissolved fraction-Extract from the Regulation on reference objectives for the classification of surface water quality of 10.12.2002 (table 6)

.

Table 6.Classification of surface water in quality classes according to ion content of the dissolved fraction-Extract from the Regulation on reference objectives for the classification of surface water quality

A.5.1.Metal ions in dissoled fraction						
	Unit	Quality class				
		I	II	III	IV	V
Zinc (Zn^{2+})	µg/l	background	5	10	25	> 25
Cupper (Cu^{2+})	µg/l	background	2	4	8	> 8
Chromium total (Cr^{3+} + Cr^{6+})	µg/l	background	2	4	10	> 10
Lead (Pb^{2+})	µg/l	background	1	2	5	> 5
Cadmium (Cd^{2+})	µg/l	background	0,1	0,2	0,5	> 0,5
Mercury (Hg^{2+})	µg/l	background	0,1	0,15	0,3	> 0,3
Nickel (Ni^{2+})	µg/l	background	1,0	2,0	5,0	> 5,0

Table 7 Classification of surface water in quality classes in sampling points in terms of the concentration of ions in the dissolved fraction

Sampling points/ Reference parameter	Tusa	Pădurea Neagră	Boghiș	Suplacu de Barcău	Marghita	Parhida
Zn II Concentration	I	I	III	III	II	II
Cu II Concentration	I	I	II	III	II	II
Pb II Concentration	I	I	I	II	I	I
Hg II Concentration	I	I	I	I	I	I
Ni II Concentration	I	I	II	II	II	II

CONCLUSIONS

Higher metals concentrations were measured during the summer period. The increase of metal ions concentrations in the studied surface waters in the summer months can be explained due to local sources of pollution such as population and industry activities. During the summer months, there was an increase in the concentration of metal ions, especially downstream of Boghiş, Suplacul de Barcău and Marghita, probably due to domestic wastewater, tourist thermal units (in the case of Boghiş Baths) and those resulting from production processes (in the case of Suplacul de Barcău and Marghita).

The smallest quantities of metal ions were registered as expected in Tusa, in the upper part of the river Barcău.

In the case of Pădurea Neagră City were registered lower concentrations of metal ions than in the case of the other investigated localities, probably due to the fact that the local industry is less represented and also because the wastewater is collected and treated in a more efficient waste water treatment plant.

In Tusa and Padurea Neagră sampling points the surface water can be classified in class I of quality regarding all metallic ions investigated. In Boghiş and Suplacul de Barcău sampling points the surface water was classified in class II and III of quality regarding some of the metallic ions investigated (Zn II, Cu II and Ni II for Boghiş and Zn II, Cu II, Ni II and Pb II for Suplacul de Barcau). At the border with Hungary (Parhida) the water of the Barcău River falls in the quality class I in terms of the content of Pb II and Hg II and in the quality class II in terms of the content of Zn II, Cu II and Ni II.

In order to prevent pollution of the Barcău River Basin, it is necessary to take measures to remove the wastewater discharge without prior treatment.

REFERENCES

1. Cîrţînă D, 2011, Aspecte privind monitorizarea calităţii apelor de suprafaţă. Analele Universităţii “Constantin Brâncuşi” din Târgu Jiu, Seria Inginerie, no. 1, pp 101;
2. Domuţa C. și colab., 2011, Relaţii în sistemul apă-sol-plantă-atmosferă în Câmpia Crişurilor, Ed. Univesităţii din Oradea;
3. Eaton A. D. and Franson M. A. H., 2005, Standard Methods for the Examination of Water & Waste Water. American Public Health Association;
4. Gavriș, G., 2003, Chimia mediilor poluante, Ed. Universității din Oradea;
5. http://www.rowater.ro/dacrisuri;
6. http://www.mmediu.ro/app/webroot/uploads/files/2016-03-24_RO8_FRMP_PMRI_CRISURI.pdf
7. http://chislaz.ro/comuna-chislaz/reteaua-hidrografica/;
8. https://www.epa.gov/;
9. https://www.iarc.who.int/;
10. Jude E, 2014, Research regarding on some Chemical Parameters of Crisul Repede Water Downstream of Oradea, Natural Resources and Sustainable Development**,** vol. 4, pp.87;
11. Pătroescu,C., Gănescu, I., Papa, I. 2000, Water Analysis, Sitech Publ., Craiova;
12. SREN ISO15586, 2004, Calitatea apei. Determinarea elementelor din urme prin spectrometrie de absorbție atomică cu cuptor de grafit;
13. Tchounwou, P.B.; Yedjou, C.G.; Patlolla, A.K.; Sutton, D.J., 2012, Heavy metal toxicity and the environment. Molecular, Clinical and Environmental Toxicology; Luch, Vol.101, pp.133-64;
14. The normative regarding the reference objectives for the classification of the surface water quality from 10.12.2002/ https://lege5.ro/Gratuit/hezteobt/clasificarea-calitatii-apei-de-suprafata-si-a-sedimentelor-normativ?dp=giztcmjzgiyta;
15. Varduca, A. 2000, Protecția calității apelor, Editura H.G.A., București.

Analele Universităţii din Oradea-Fascicula Chimie, Vol. XXVIII(28), 2021

COUMARIN DERIVATIVES WITH POTENTIAL ANTIMICROBIAL ACTIVITY. IN SILICO STUDIES

Paul Andrei NEGRU[1], Georgeta ȘERBAN[1]
[1]University of Oradea, Faculty of Medicine and Pharmacy, Pharmaceutical
Chemistry Department, 29 Nicolae Jiga, 410028 Oradea, Romania

Abstract. *The discovery of antibacterial and antifungal compounds has improved clinical outcomes in almost all infections. Therefore in our studies we tried to analyze the applicability of molecular docking in predicting the pharmacological effects of some coumarin compounds synthesized in our laboratory.*

Key words: molecular docking, coumarin derivatives

INTRODUCTION

Antimicrobial agents are one of the most remarkable examples of progress in modern medicine. Many infectious diseases, which were once considered incurable and potentially lethal, can now be effectively treated with antibiotics. The discovery of antibacterial and antifungal compounds has improved clinical outcomes in almost all infections [1]. The biggest step in this field was taken in 1942 with the discovery of penicillin, and after that the lethality of some infections decreased by up to 70% [2]. Antimicrobial agents are one of the most powerful tools for fighting life-threatening infections. Antimicrobial resistance - the ability of pathogens to inactivate the drugs designed to kill them - is currently one of the greatest public health challenges in the world [3, 4].

The chemical approach to the development of new compounds is a good strategy. Unfortunately, this has begun to fail because the pharmaceutical industry has lost the interest in developing new drugs since finding new compounds is a difficult and extremely expensive process. Molecular docking is an in-silico approach to drug development that allows predictions of how ligands can interact with proteins. The greatest benefit of molecular docking is the low cost of these studies. By further improving the algorithms by which molecular docking is performed, this method could become a powerful tool for drug discovery in the future [5]. Therefore in our studies we tried to analyze the applicability of molecular docking in predicting the pharmacological effects of some coumarin compounds synthesized in our laboratory.

MATERIALS AND METHODS

The docking studies were conducted using AutoDockTools version 1.5.6, the graphical user interface for AutoDock [6]. Discovery studio was used to obtain the 2D diagrams of the interactions betwen the ligand and protein [7].

The docking studies included two target proteins – DNA-gyrase (PDB ID: 2XCT) of *Staphylococcus aureus* [8] and lanosterol 14-alpha demethylase of *Candida albicans* (PDB ID: 5V5Z) [9]. The structures of these proteins were obtained from the protein data bank (https://www.rcsb.org/). The protein preparation consisted in removing all the water molecules and ligands in Molegro molecular viewer 2.5 and in adding polar hydrogen atoms and Gasteiger charges using AutoDockTools [10]. Ligand preparation consisted in obtaining the SDF (structure-data file) format of the ligand in ChemDraw Ultra, converting the SDF file to a PDB file using https://cactus.nci.nih.gov/translate/. The Gasteiger charges and defining all rotable bonds was done using AutoDockTools. Other settings were as default for both the ligands and proteins.

RESULTS AND DISCUSSION

Nineteen coumarin derivatives belonging to 3-(5-mercapto-4-R-1,2,4-triazol-3-yl)coumarin, 3-(5-arylamino-1,3,4-thiadiazol-2-yl)coumarin and 3-(5-arylamino-1,3,4-thiadiazol-2-yl)-6-nitrocoumarin series were synthesized and tested *in vitro* for the antimicrobial activity on the following test strains: *Stahylococcus* *aureus*, *Escherichia coli*, *Proteus vulgaris*, *Klebsiella pneumoniae*, *Pseudomonas aeruginosa* and *Candida albicans* [11, 12, 13]. To better understand the mechanism of interaction between the microbial proteins and their inhibitors, the most active compound 3-[4-(4-bromophenyl)-5-mercapto-4*H*-1,2,4-triazol-3-yl]coumarin (**C**) was subjected to molecular docking studies. In addition, two structural derivatives of this compound, 3-[4-(4-bromophenyl)-5-methylmercapto-4*H*-1,2,4-triazol-3-yl]coumarin (**D1**) and 3-[4-(4-bromophenyl)-5-acetylmercapto-4*H*-1,2,4-triazol-3-yl]coumarin (**D2**) (Fig. 1) were selected to examine whether structural modifications would have an impact on the binding site of coumarin to microbial proteins and/or on the binding energy.

To validate the docking method, a ligand model of Ciprofloxacin for 2XCT and a model of Itraconazole for 5V5Z, respectively, was built and docked into the crystal structure of the target enzyme. The docked ligand model was superimposed on the reference model of ligand taken from the protein data bank using PyMol [14]. Root mean square deviation (RMSD) between the co-crystallized ligands and the docked ligands showed values that are within the generally accepted values in the literature [15, 16].

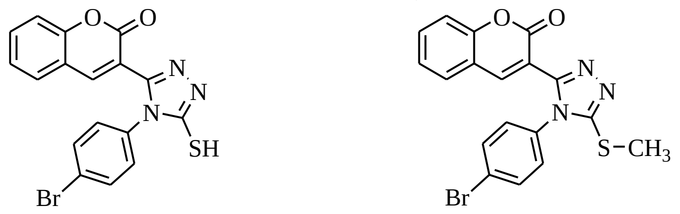

3-[4-(4-bromophenyl)-5-mercapto-4*H*-1,2,4-triazol-3-yl]-2*H*-chromen-2-one

(**C**)

3-[4-(4-bromophenyl)-5-(methylthio)-4*H*-1,2,4-triazol-3-yl]-2*H*-chromen-2-one

(**D1**)

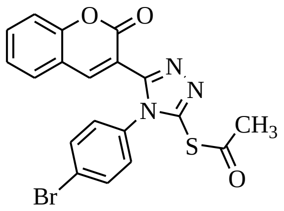

3-[4-(4-bromophenyl)-5-acetylmercapto-4*H*-1,2,4-triazol-3-yl]-2*H*-chromen-2-one

(**D2**)

Fig. 1. The chemical structures of the studied compounds.

Docking studies of coumarin derivatives on DNA gyrase 2XCT

Molecular docking studies have shown that **C** derivative has the highest affinity for the 2XCT protein. The calculated binding energy of the most stable complex of compound **C** with DNA gyrase is -8.4 kcal/mol, closely followed by derivative **D1** (-8.3 kcal/mol). Compound **D2** showed a slightly lower affinity with a binding energy of -7.7 kcal/mol. All the compounds have a good affinity for the target protein that can be compared to that of Ciprofloxacin (-8.1 kcal/mol for the Ciprofloxacin-DNA gyrase complex). However, *in vitro* experimental studies have shown that compound **C** has no activity against *Staphylococcus aureus*, which allows us to assume that other molecular mechanisms are also involved in establishing the antimicrobial activity of this compound [13].

Analyzing the 2D diagrams it can be seen that Ciprofloxacin binds to the amino acids PHE1123, ARG1122, HIS1081, PRO1080 and LYS581. Compound **C** binds to PHE1123, ARG1122, PRO1080, TYR1150, LYS1066, GLU1125, LYS581 and compound **D1** binds to PHE1123, ARG1122, PRO1080, MET1075, LYS1066, GLU1125, LYS581, TYR1150. These three compounds have in common the amino acids PHE1123, ARG1122, PRO1080 and LYS581 in their charts (Fig. 2, Table 1).

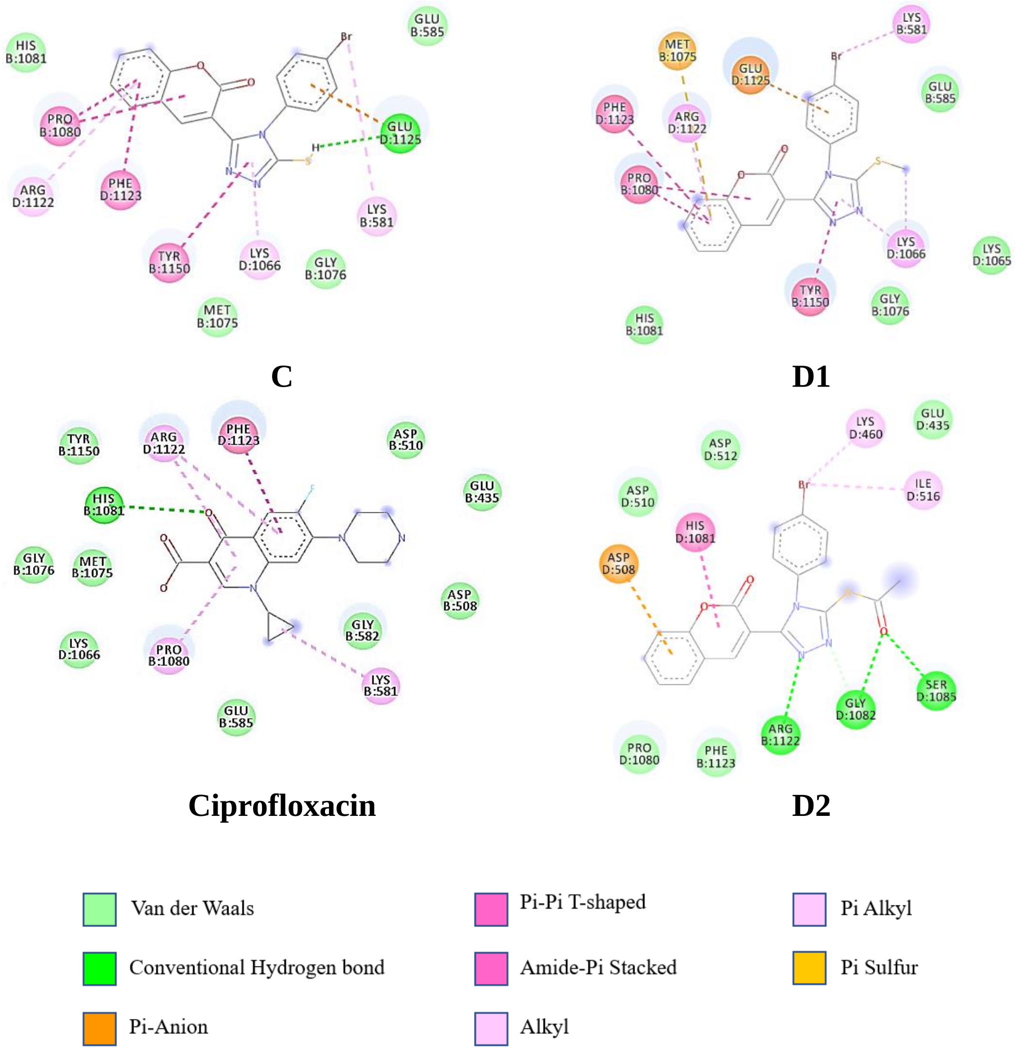

C **D1**

Ciprofloxacin **D2**

Figure 2. *Coumarin derivatives-2XCT and Ciprofloxacin-2XCT interactions*

Table 1. *Binding amino acids in the coumarins-2XCT and Ciprofloxacin-2XCT complexes*

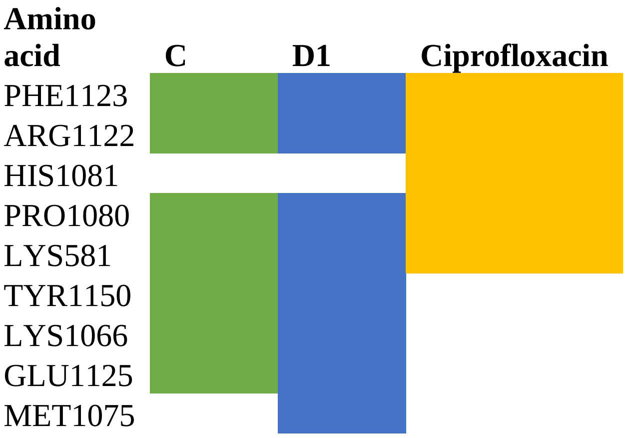

Amino acid	**C**	**D1**	**Ciprofloxacin**
PHE1123	🟩	🟦	🟨
ARG1122	🟩	🟦	🟨
HIS1081			🟨
PRO1080	🟩	🟦	🟨
LYS581	🟩	🟦	🟨
TYR1150	🟩	🟦	
LYS1066	🟩	🟦	
GLU1125	🟩	🟦	
MET1075		🟦	

In addition, the two-dimensional diagrams show that **C**, **D1** and Ciprofloxacin have a similar binding mechanism to 2XCT protein, as both Ciprofloxacin and the two coumarin compounds bind to the amino acids PHE1123, ARG1122 and PRO1080 through the two condensed hexacycles in their structures which can also be seen when the protein-ligand complex of each compound overlaps (Fig. 3). Derivative **C** has a higher affinity for the receptor, which may be due to the hydrogen bond formed between the thiol -SH group and the glutamic acid GLU1125 at the active site of the enzyme which can not be possible for the substituted derivative **D1**

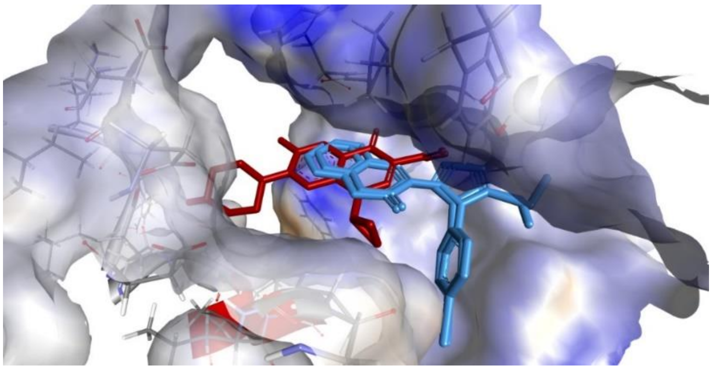

Figure 3. *Coumarins at the 2XCT protein binding site, three-dimensional model. Overlapping ligand-protein complex: red – Ciprofloxacin, blue – compounds* ***C*** *and* ***D1***

Compound **D2** has the lowest affinity for the protein (-7.7 kcal/mol). In addition, the binding site of this ligand is different from the binding site of the other compounds (Fig. 4). Compound **D2** interacts with the following amino acids: ASP508, HIS1081, LYS460, ILE516, SER1085, GLY1082 and ARG1122 and has only two common amino acids with ciprofloxacin: HIS1081, ARG1122. This may be due to the steric hindrance developed by the acetylmercapto -$SCOCH_3$ group in D2, which made it difficult to bind the substance to the active site of the enzyme.

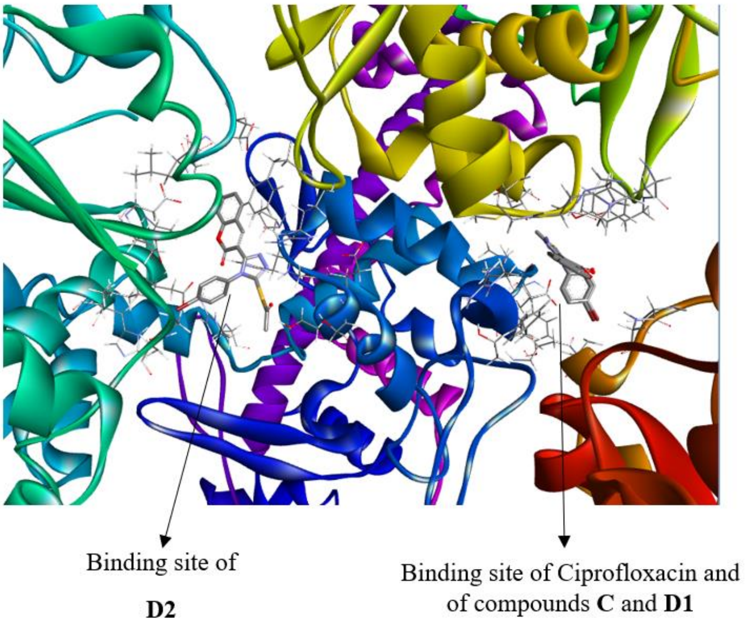

Figure 4. *Coumarin derivatives* ***C****,* ***D1*** *and* ***D2*** *at the 2XCT protein binding sites.*

Docking studies of coumarin derivatives on lanosterol 14α-demethylase 5V5Z

Itraconazole possesses a bulky molecule, which makes possible many interactions between the drug molecule and the target enzyme and a good afinity for protein (-10.9 kcal/mol). The most stable conformation of compound **C** had the binding affinity of -8.8 kcal/mol, while for the compound **D2** the binding energy value was -7.7 kcal/mol. Derivative **D1** showed the highest affinity for the protein with a calculated binding energy of the most stable complex of -9.0 kcal/mol. Therefore the derivative **D2** showed the lowest binding affinity and also showed a different binding site compared to the other three compounds.

Itraconazole binds to the amino acids GLY65, TYR64, HIS377, PRO230, MET508, TYR118, ILE304, ILE131, LYS143, LEU139, LEU300 and LEU376. Compound **C** binds to PHE475, ILE304, GLY308, PHE228, PHE126, CYS470 and ILE471, while the compound **D1** binds to ILE131, ILE304, LEU376, ILE379, LEU121, TYR118 şi TYR132. All three compounds bind to ILE304, while Itraconazole and **D1** have also in common the amino acids TYR118, ILE131 şi LEU376. All compounds have an 1,2,4-triazole ring in their molecules which could be the reason why coumarins show a high binding affinity to 5V5Z (Fig. 5, Table 2).

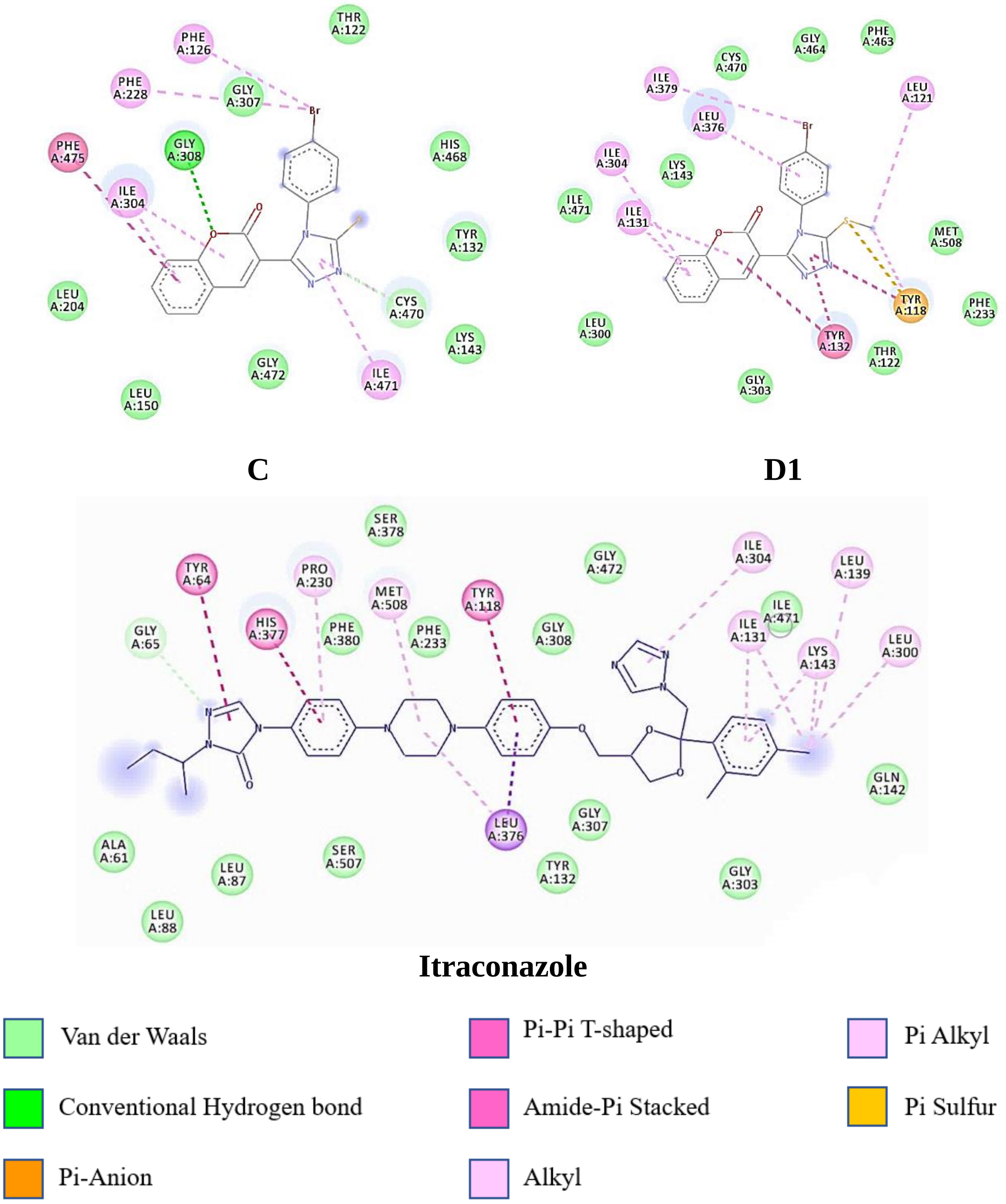

C **D1**

Itraconazole

Figure 5. Coumarins-5V5Z and Itraconazole-5V5Z interactions

When the most stable conformation of Itraconazole overlaps the conformation of derivatives **C** and **D1**, respectively, it can be seen that the protein binding sites overlap in certain areas. It can be predicted that by adding more bulky substituents to compound **C**, especially on the 1,2,4-triazole ring, derivatives with a higher affinity for lanosterol 14α-demethylase could be obtained. A complete overlap is unlikely, due to the fact that itraconazole is a much larger molecule and has more torsion angles compared to compounds **C** and **D1** (Fig. 6).

Table 2. Binding amino acids in the coumarins-5V5Z and Itraconazole-5V5Z complexes

Amino acid	**C**	**D1**	**Itraconazole**
GLY65			🟨
TYR64			🟨
HIS377			🟨
PRO230			🟨
MET508			🟨
TYR118		🟦	🟨
ILE304	🟩	🟦	🟨
ILE131		🟦	🟨
LYS143			🟨
LEU139			🟨
LEU300			🟨
LEU376		🟦	🟨
PHE475	🟩		
GLY304	🟩		
PHE228	🟩		
PHE126	🟩		
CYS470	🟩		
ILE471	🟩		
ILE379		🟦	
LEU121		🟦	
TYR132		🟦	

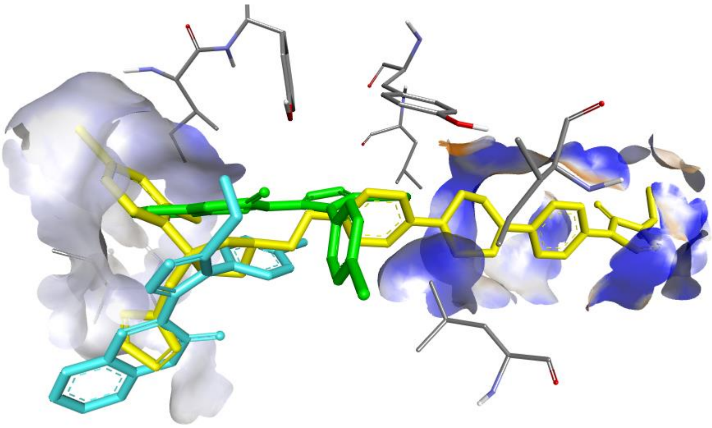

Figure 6. *Coumarins at the 5V5Z protein binding site, three-dimensional model. Overlapping ligand-protein complex: yellow – Itraconazole, blue – compound **C** and green – compound **D1***

CONCLUSIONS

The docking studies of derivatives **C**, **D1** and **D2** on 2XCT protein (AND-gyrase) showed the compound **C** as the most effective ligand. The *in vitro* antimicrobial study of compound **C** showed that it does not act on *Staphylococcus aureus* strains, however the compound had good activity against some Gram-negative germs, such as *Pseudomonas aeruginosa*. Docking the compounds to the 5V5Z protein (lanosterol 14α-demethylase) highlighted **D1** as the most active, with a slight increase in affinity for the protein. However, the derivatives **C** and **D1** have very close affinity. Derivative **C** showed *in vitro* antifungal activity against *Candida albicans* strains. Although it is not known whether coumarins can inhibit the enzyme lanosterol 14α-demethylase, the docking studies demonstrated a good affinity of the studied compounds for this protein.

The binding values of **D2** (-7.7 kcal/mol for both D2-DNA gyrase and D2-lanosterol 14α-demethylase complexes) and also the binding sites showed no similarities with compounds **C** and **D1**. The results did not show any significant increase in the affinity of coumarins for the target proteins after chemical modifications. The derivatives might possess chemotherapeutic potential. These studies will be followed by *in vitro* experiments to validate our findings from the in silico studies.

References

1. Kon K., Ray M., Antibiotic Resistance: Mechanisms and New Antimicrobial Approaches, 1st edition, Academic Press, Elsevier, 2016.
2. Spizek J., Novotna J., Rezanka T., Demain A. L., Do we need new antibiotics? The search for new targets and new compounds, J. Ind. Microbiol. Biotechnol., 2010, 37(12), 1241-1248.
3. Davies J., Dorothy D., Origins and evolution of antibiotic resistance, Microbiol. Mol. Biol. Rev., 2010, 74(3), 417-433.
4. Antibiotic/Antimicrobial resistance (AR/AMR), Centers for Disease Control and Prevention, https://www.cdc.gov/drugresistance/about.html, accessed at 6th October 2021.
5. Berry M., Fielding B., Gamieldien J., Practical Considerations in Virtual Screening and Molecular Docking, Emerging Trends in Computational Biology, Bioinformatics, and Systems Biology, 2015, 487-502. doi:10.1016/b978-0-12-802508-6.00027-2
6. Sanner M.F., Python: a programming language for software integration and development, J. Mol. Graph. Model, 1999, 17(1), 57-61.
7. Discovery Studio Dassault Systemes BIOVIA, Discovery studio, v19.1.0.18287, San Diego: Dassault Systemes, 2020.
8. Bax B.D., Chan P.F., Eggleston D.S., Fosberry A., Gentry D.R., Gorrec F., Giordano I., Hann M.M., Hennessy A., Hibbs M., Huang J., Jones E., Jones J., Brown K.K., Lewis C.J., May E.W., Saunders M.R., Singh O., Spitzfaden C.E., Shen C., Shillings A., Theobald A.J., Wohlkonig A., Pearson N.D., Gwynn M.N., Type IIA topoisomerase inhibition by a new class of antibacterial agents, Nature, 2010, 466(7309), 935-940. doi:10.1038/nature09197
9. Keniya M.V., Sabherwal M., Wilson R.K., Woods M.A., Sagatova A.A., Tyndall J.D.A., Monk B.C., (2018). Crystal structures of full-length lanosterol 14α-demethylases of prominent fungal pathogens *Candida albicans* and *Candida glabrata* provide tools for antifungal discovery, Antimicrob. Agents Chemother., 2018, 62(11):e01134-18, doi:10.1128/AAC.01134-18.

10. Trott O., Olson A.J., AutoDock Vina: improving the speed and accuracy of docking with a new scoring function, efficient optimization and multithreading, J. Comput. Chem., 2010, 31(2), 455-461.
11. Şerban G., Coman M., Curea E., Proinov L., Obţinerea şi caracterizarea unor cumarine heterociclice, Farmacia, 49(2), 45-52, 2001.
12. Şerban G., Suciu A., Crişan O., Coman M., Curea E., Sinteza şi studiul fizico-chimic al unor 3-(5-mercapto-4-R-1,2,4-triazol-3-il)cumarine, Farmacia, 2002, 50(5), 22-28.
13. Şerban G., Matinca D., Bradea O., Gherman L., Coman M., Curea E. Studiul activităţii biologice a unor cumarine heterociclice, Farmacia, 53(2), 91-99, 2005.
14. PyMOL Molecular Graphics System, Version 2.2.3 Schrödinger, LLC. https://pymol.org/2/
15. Costa J.S., Ramos R.S., Costa K.S.L., Brasil D.S.B., Silva C.H.T.P., Ferreira E.F.B., Borges R.S., Campos J.M., Macedo W.J.C., Santos C.B.R., An in silico study of the antioxidant ability for two caffeine analogs using molecular docking and quantum chemical methods, Molecules, 2018, 23(11), 2801-2817.
16. Cole J.C., Murray C.W., Nissink J.W.M., Taylo R. D., Taylor R., Comparing protein-ligand docking programs is difficult. Proteins, 2005, 60(3), 325-332.

Analele Universităţii din Oradea-Fascicula Chimie, Vol. XXVIII(28), 2021

EFFECT OF CU^{2+} AND ZN^{2+} INCORPORATED INTO FLUOROHYDROXIAPATITE COATING ON CoCrMo ALLOY WITH ANTIMICROBIAL PROPERTIES

Mariana PRODANA[1] , Daniela IONITA[1*] , Mihai ANDREI [2,3], Madalina SIMOIU[4]

1.University Politehnica of Bucharest, Faculty of Applied Chemistry and Materials Science, 1-7 Polizu, 011061, Bucharest, Romania,
md_ionita@yahoo.com
2. Elias University Emergency Hospital Bucharest, 17 Marasti Blvd., 011461, sector 1 Bucharest, Romania;
3 UMF Carol Davila Str Dionisie Lupu 37, sect 2, 020021, Bucharest,
4.National Institute for Infectious Diseases “Prof. Dr. Matei Balş”, Dr. Calistrat Grozovici Street 1, Bucharest 021105, Bucharest, Romania;

Abstract.*The present study reflected antibacterial properties of a coating based on fluorohydroxyapatite (FHA)/with Cu^{2+} and Zn^{2+} ions on CoCrMo alloy in phosphate buffered saline (PBS) medium. The coating structure was identified by Fourier transformed infrared spectroscopy (FTIR) and the surface analysis of phosphate deposits by quantifying the hydrophilic / hydrophobic balance and the roughness by AFM determinations.Cu^{2+} and Zn^{2+} ion release was studied using inductively coupled plasma mass spectrometry (ICP-MS) method. Antibacterial properties of coatings were determined by contact method using using agar disc diffusion method for two bacterial strains: Staphyloccoccus aureus and Pseudomonas aeruginosa.*

Keywords: ion release, antibacterial effect, fluorohydroxyapatite, FTIR, ICP-MS.

1.INTRODUCTION

Strating to 1900’s, the scientific community become interested in founding new materials for bone substitution in biomedical field [1].The interest of researchers was attracted to materials based on Ca and P so, in 1920 appeared the first article that used such materials as fillers of bone defects in rabbits [2]. Bone infections represented for many years an important subject in medicine.

Having that aim, it was looked for materials with properties close to those of human bone that could replace parts of the infected bone or that could contribute to the growth of bone material on certain portions of bone. Due to their mechanical properties similar to bone and due to the osteogenic properties, CaPs is today used in different fields, for orthopedics, for the treatment of bone fractures, for implantology, for dentistry and for maxillofacial reconstruction [3,4].

Hydroxiapatite belongs to the group of apatites, (HA, $Ca_{10}(PO_4)_6(OH)_2$), represent the inorganic part of the bone and contain Ca and P in a ratio close to 1.67 [5]. HA presents very good biocompatibility, bioactivity, and biodegradability, beeing used as implant material, for drugs relase, for bone cement, for hybrid material together with carbon nanotubes in order to increase the strenth [6] with applications in biomaterials field and medicine.Another type of apatite isfluorapatite (FA; $Ca_{10}(PO_4)_6F_2$) beeing more stable from chemical and structural point of view than hydroxyapatite and forms the outer layer of teeth [7,8].

Doped phosphate masses introduce into the crystal structure of hydroxyapatite various ions which have the role of improving its properties. The deposition of fluorohydroxyapatite, $Ca_{10}(PO_4)_6(OH)_{2-x}F_x$, where 0 <x <2, represents the degree of fluorination, is a method that was initially developed for the titanium substrate, but in the present paper an attempt was made, to extend it to coating of substrates as Co-Cr-based alloys. The introduction of the F$^-$ ion, which replaces some HO$^-$ groups, has proven to be beneficial because it provides a better degree of coating of the substrates, a higher stability in terms of its dissolution in various media and a better cellular response [9].

This article proposes the introduction of copper ions (Cu^{2+}) and zinc (Zn^{2+}) in the structure of fluorohydroxyapatite in order to increase the animicrobial effect.Copper is an element that can be easily metabolized [10] and has a low cellular toxicity, as well as a high degree of biocompatibility [11], the surfaces coated with this metal having a very high antibacterial effect [12] and the antimicrobial properties of zinc oxides are well known, it has been used for a long time, especially in dentistry [13].

Heavy metals are toxic and react with proteins, therefore bonds are formed with protein molecules. As a result, cellular metabolism is inhibited causing the death of microorganisms [12].

ZnO nanoparticles have an antibacterial effect on both *Gram-positive* and *Gram-negative* bacteria. They have an antibacterial effect even on spores that are resistant to high temperatures and pressures [13]. Adhesion of ZnO particles to bacterial membranes may be the cause of zinc toxicity to bacteria [14].

Infections produced post-implantation are often the main cause of surgery failure, so implantable materials must tend at the time of implantation to an antibacterial effect and at the same time have a high degree of cytocompatibility [15]. There are many bacteria that can cause such problems, but among the most common are *Staphyloccoccus aureus* and *Pseudomonas aeruginosa*. Methicillin-resistant *Staphyloccoccus aureus (MRSA)* is resistant to all β-lactam antibiotics, but there have been results that have demonstrated an antimicrobial effect of copper on *MRSA* [16]. Infections with *Pseudomonas aeruginosa* or the pyocyanic bacillus are often difficult to treat, so in addition to antibiotics, numerous therapeutic options have been explored, including even quorum-sensing inhibitors [17].

2.MATERIALS AND METHODS

2.1.Materials. Sample preparations

For the deposition of the coatings it was used CoCrMo alloy as substrate. The CoCrMo alloys samples, cut with a diameter of 1.6 mm and a thickness of 2 mm, were preprepared by polishing with a 600 and 1200-grit SiC paper, ultrasonically cleaned in acetone and double distilled water.

For the deposition of doped and non-doped fluorohydroxyapatite with copper and zinc ions, the electrochemical deposition method was chosen.Electrochemical deposition is an efficient and easy to use method in laboratory conditions, so it was chosen to obtain this type of protective coating, another criterion being that unlike other more complex methods (hot spraying or laser deposition), electrochemically deposited phosphate masses have a structure much more similar to the natural ones found in the composition of bone tissue [18].

This method uses a conventional electrochemical cell with three electrodes: the reference electrode (Ag/AgCl), the platinum auxiliary electrode and the working electrode formed of the material chosen as substrate.

The composition of the metal plates, according to the technical data sheet, used as working electrodes are found in Table 1, the sample were immersed in an electrolyte whose composition is found in Table 2, and whose pH was adjusted to 4.8 by adding HCl.

The composition of CoCrMo is presented in Table 1.

Table 1. Composition ranges for CoCrMo alloy.

Substrate	Cr	Mo	Ni	Mn	Si	N	C	P	S	Co	Fe
CoCrMo (%)	27.00	5.5	0.99	1.00	1.00	-	-	-	-	63.5	2.22

Table 2. Composition of the electrolyte used in the deposition process.

No.	Component	Concentration (mol/L)	Amount (g)
1	$(NH_4)_2HPO_4$	0.025	1.6482
2	$CaCl_2 \cdot 2H_2O$	0.042	3.0874
3	NH_4F	0.012	0.2222

In order to improve the electrodeposition process, in order to obtain a dense coating due to the release of H_2 and the production of HO^-, 3% H_2O_2 was added to the prepared solution, in a ratio of 1:10 to the electrolyte. The concentration of each component was chosen so as to ensure a Ca/P ratio of approximately 1.67. To the prepared electrolyte were added 50 ppm $ZnCl_2$ to obtain Zn^{2+} doped fluorohydroxyapatite, 50ppm $CuCl_2 \cdot 2H_2O$ to obtain Cu^{2+} doped fluorohydroxyapatite, and 50 ppm mixture of $ZnCl_2$ and $CuCl_2 \cdot 2H_2O$ to obtain fluorohydroxy type of ions. The working conditions was: curent density 1mA/cm2 for 30 min at 370C, followed by heat treatment at 130^{0}C for 360 min.

Chronopotentiometry, in PULSE mode usinga VoltaLab 4 potentiostat/galvanostat, PGZ 301 model, from Radiometer Analytical, was used as a method, and the curves were recorded with the Volta Master 4 software. During the entire deposition period, for 30 minutes, the cathodic current density was kept constant at a value of 1 mA/cm^2, with a measurement step of 0.5 seconds.

2.2.Structural characterization (FTIR) of fluorohydroxyapatite coatings doped with Cu and Zn ions and undoped

The spectra of the systems investigated by IR absorption were recorded at room temperature using using a Spectrum 100 Series FTIR Spectrometer from Perkin Elmer.

Have been reported in the literature FTIR spectra where hydroxyapatite shows absorption peaks specific to the hydroxyl group at 631 and 3573cm^{-1} [19].In the spectra, obtained in the present study, Figure 1, these peaks do not appear, which indicates that these two vibrations, specific to the OH^- group are disturbed by the introduction of fluoride ions into the hydroxyapatite network [20], moreover their lack clearly indicates that fluoride ions have been successfully incorporated into the apatite matrix.

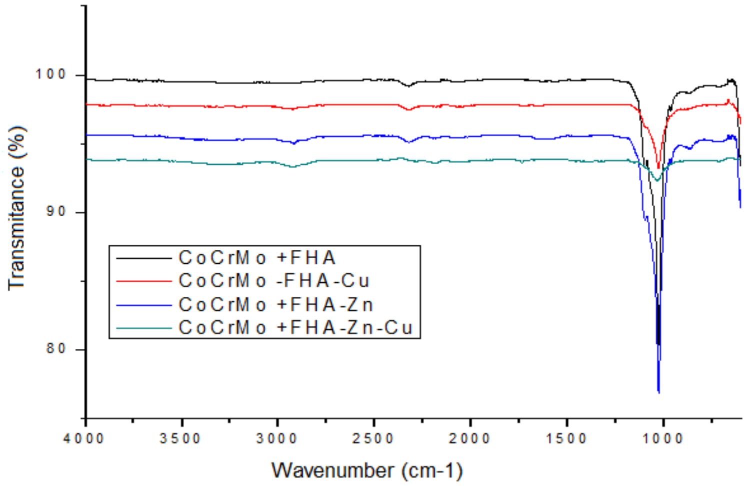

Figure 1. *FTIR spectra of CoCrMo+FHA, CoCrMo+FHA-Cu, CoCrMo+FHA-Zn, CoCrMo+FHA-Zn-Cu samples.*

The peaks that appear in the interval 924-966cm^{-1} are due to the asymmetric tensile vibrations of the P-O-P bonds joined with large metaphosphate rings, and the main peak appeared in the interval of 1001-1077cm^{-1}, together with another adjacent peak, less obvious, located in the same interval, due to the asymmetric tensile vibrations of the P-O-P bonds joined with small metaphosphate rings.

Peaks that appeared in the range 1070-1093cm^{-1}, are attributed to the asymmetric tensile vibrations of the PO^{2-} groups, those in the range 1157-1183cm^{-1} come from the terminal phosphate groups PO_3^{2-}.

The peaks appeared around 603cm^{-1} is attributed to the deformation vibrations of PO_4^{3-} [21], and the band formed around 2320 cm^{-1} can be attributed to an elongation vibration of the O-H bond associated with hydrogen bonds. The band at about 1265cm^{-1} is attributed to the tensile vibrations of the oxygen double bond, (P = O). At 1640cm^{-1} there are vibrations of deformation of the bonds of H_2O free molecules.

2.3.Surface analysis: hydrophilic / hydrophobic balance and AFM determinations

To evaluate the hydrophilic-hydrophobic character, wettability measurements were performed on the modified surfaces, by determining the contact angle (CA) using the 100 Optical Contact Angle Meter-CAM100.

Each value for determining the contact angle is the average of three measurements. The tests were performed with an accuracy of ± 1°C to 25°C. The results are presented in Table 3. The surface roughness (Ra) of the samples was evaluated with an atomic force microscope at APE A.P.E. Research Company, using the contact mode.

Table 3. Contact angle (CA) values and surface energy values (SGE) on the CoCrMo substrate

Sample	CA	SFE (mJ/m^2)
CoCrMo/FHA	28±0.66	64±0.37
CoCrMo/FHA-Cu	36±0.61	59±0.32
CoCrMo/FHA-Zn	39±0.59	57±0.34
CoCrMo /FHA-Cu-Zn	42±0.55	54.9±0.39

The measurements did not show significant differences between the roughness values of the sample surfaces covered with doped fluorohydroxyapatite. The reduced contact angle reveals the increased surface roughness as well as its hydrophilic character. The hydrophilic character of the coating, as seen from the low values of the contact angle should be a support for promoting osteogenesis, electrodeposited phosphate masses will promote the growth of osteoblasts. However, there is a very slight increase in its value in the case of doped fluorohydroxyapatite, compared to undoped hydroxyapatite.

2.4. Ions release from the deposited coatings

The ICP-MS technique was used, both, to determine the Zn and Cu content, as well as to determine the rate of detachment of these ions from the film deposited on CoCrMo substrates.

Ion release was determined using ICP-MS, a sensitive method that can detect a wide range of elements with a concentration of up to nanograms per liter (ppb; parts per billion) and even lower. The ICP-MS-equipment was a Perkin Elmer ELAN DRC-e instrument that uses the introduction of a liquid sample by a micro-nebulizer. Calibration was performed using a multi-element aqueous solution for internal standardization. All results presented are the average of three read measurements against blank. Analytical quality control was monitored by several blank readings, unknown samples, and NIST (National Institute of Standards and Technology) 1643e certified reference material, IAEA W4.

To determine the Zn and / or Cu content of the coatings deposited on CoCrMo, the samples were treated with nitric acid to dissolve the deposited layer. The CoCrMo sample coated with FHA-Cu-Zn was immersed in phosphate buffered saline (PBS) in sterile polystyrene vials for 2, 24, 48, 72 hours at 37°C. The composition of the solution was: 8 g / L NaCl , 0.2 g / L KCl, 1.15 g / L Na_2HPO_4, and 0.2 g /L KH_2PO_4, according to ASTM F2129 standard [22].

In the case of the CoCrMo sample coated with FHA-Zn-Cu, in the first 2 hours of immersion, there was a rapid release of Cu ions reaching 0.25ppm. In the next 22 hours the release of Cu ions was slowed down so that after 24 hours it reached only 0.38 ppm. During the other 48 hours of monitoring the concentration of Cu ions detected remains constant, around 0.48 ppm. For Zn ions released from the FHA-Zn-Cu coating, a much slower release was recorded than in the case of copper ions, so that after 24 hours of immersion 0.001 ppm of Zn ions were recorded, the release continuing slowly until at the 72 hours of testing, after this period being registered in the test solution 0, 03 ppm Zn. The evolution of ion release is illustrated in Figure 2.

The lethal dose of copper (LD50) according to the literature [23] is 46 mg/L after 24 hours of incubation for L929 mouse fibroblasts, while zinc assumes variations in concentration between 10 and 250 mg/L [24, 25].

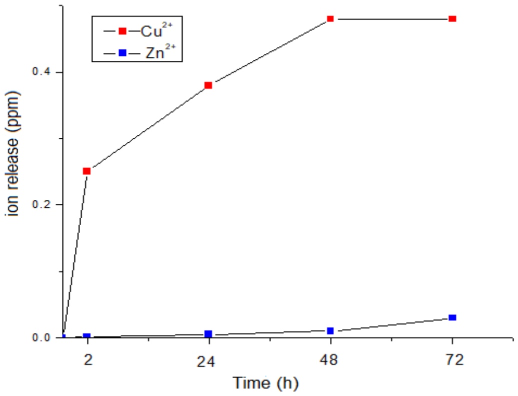

Figure 2. *Evolution of ion release over time for FHA-Zn-Cu coated CoCrMo sample.*

2.5. Antibacterial activity of the deposited coatings

Antibacterial activity was determined by calculating bacterial growth inhibition using formula (1), where (T_0 and T_1 at time 0 and 24 hours) and positive control(C_0 and C_1 at time 0 and at 24 hours)[9].

$$I\% = \frac{(C_1-C_0)-(T_1-T_0)}{(C_1-C_0)} \times 100 \qquad (1)$$

It was used two ATCC reference strains, *Gram-positive* and *Gram-negative* bacteria that cause infections after implantation. *Staphyloccoccus aureus* and *Pseudomonas aeruginosa* were cultured aerobically 24 hours at 37°C on Columbia agar plates-5% ram's blood. From the fresh cultures, 3-4 colonies were selected and inoculated in standard saline solution from Fresenius Kabi. The concentration was adjusted to 0.5 McFarland units, meaning approximately 1.5x108CFU. For each bacterial strain the samples were placed in sterile glass tubes with a diameter of 18 mm, over which were poured 10ml of infected medium. In the positive control tube was placed only infected medium, and in the negative control tube was placed only solution. saline. The tubes were incubated for 24 hours at 37 ° C with gentle shaking from time to time[26, 27].

The optical densities were read at 600 nm using a Jenway UV – VIS spectrophotometer. The level of inhibition is shown in Table 5. The results presented are the average of five readings.

Table 5. *Bacterial growth inhibition indices for coatings deposited on the CoCrMo substrate.*

Sample	CoCrMo /FHA	CoCrMo/ FHA-Cu	CoCrMo/ FHA-Zn	CoCrMo/ FHA-Zn-Cu
I% S.aureus	5.03 ±0.12	68.22 ±1.02	67.56±2.14	66.43±1.84
I% P.aerug	5.51 ±0.11	59.12 ±1.08	53.21±1.88	54.03±1.76

In all the cases of using cooper, zinc or both ions for doping FHA, the level of inhibition is much higher that the one obtained for the undoped FHA.

In the case of FHA-Cu the level of inhibition islittle higher than in the case ofCoCrMo/FHA-Znfor both *Gram-negative* and *Gram-positive* bacteria.The highest value of the degree of inhibition is obtained in the case of the double sample doped with Cu ions and Zn ions, which indicates the synergistic effect of the two ions added in FHA in terms of antimicrobial effect.

3.CONCLUSIONS

Using electrochemical deposition method, it was obtained doped and undoped FHA. The samples were characterized using FTIR, putting in evidence the success of obtaining the materials of interest. Using contact angle,it wasdetectedfor every sample an hydrophilic character of the coating, a good aspect for promoting the growth of the osteoblast, the samples that were doped with cooper and zinc ions presented a very slight increase of the contact angle compared to undoped hydroxyapatite.

The stability of the coatings, by ICP-MS put in evidence a small rate of detachment of ions from the film deposited on CoCrMo substrates, which is an indication of stability of the coatings.

By doping Cu^{2+} and Zn^{2+} in a FHA/CoCrMo sample, we obtain some benefits likea good antimicrobial effect. The highest degree of inhibition is obtained in the case of CoCrMo/ FHA-Zn-Cu, which indicates the synergistic effect of the two ions, Zn^{2+} and Cu^{2+} added in FHA in terms of antimicrobial effect. The results obtained indicate a good stability and a very good antibacterial effect a promising result of the use of such materials in bio-applications.

REFERENCES

[1] Fiume, E.; Magnaterra, G.; Rahdar, A.; Verné, E.; Baino, F. Hydroxyapatite for Biomedical Applications: A Short Overview. Ceramics 2021, 4, 542–563. https://doi.org/10.3390/ceramics4040039

[2] Albee, F.H.; Morrison, H.F. Studies in bone growth triple calcium phosphate as a stimulus to osteogenesis. Ann. Surg. 1920, 71, 32–39.

[3] Jazayeri, H.E.; Rodriguez-Romero, M.; Razavi, M.; Tahriri, M.; Ganjawalla, K.; Rasoulianboroujeni, M.; Malekoshoaraie, M.H.;Khoshroo, K.; Tayebi, L. The cross-disciplinary emergence of 3D printed bioceramic scaffolds in orthopedic bioengineering.Ceram. Int. 2018, 44, 1–9.

[4] Jeong, J.; Kim, J.H.; Shim, J.H.; Hwang, N.S.; Heo, C.Y. Bioactive calcium phosphate materials and applications in bone regeneration. Biomater. Res. 2019, 23, 4.

[5] Irfan, Mohammad & Irfan, Masooma & Zaman, Shafiq Uz & Zaman, Muhammad Khaliq U & Muhammad, Nawshad. (2020). Overview of hydroxyapatite; composition, structure, synthesis methods and its biomedical uses. 6. 84-99.

[6] M. Prodana, M. Duta, D. Ionita, D. Bojin, M. Stan, A. Dinischiotu, I. Demetrescu, A new complex ceramic coating with carbon nanotubes, hydroxyapatite and TiO2 nanotubes on Ti surface for biomedical applications. Ceramics International, 2015, 41(5), p. 6318-6325.

[7] N Montazeri, R Jahandideh, Esmaeil Biaza, Synthesis of fluorapatite–hydroxyapatitenanoparticles and toxicity investigations, International Journal of Nanomedicine 2011:6 197–201.

[8] Sanosh KP, Chu M-C, Balakrishnan A, et al. Synthesis of nanohydroxyapatite powder that simulate teeth particle morphology and composition. Curr Appl Phys. 2009;9(6):1459–1462.

[9] P. Vijayan, M. Thomas, K.C. George, “Effect of calcinations on electrical properties of TiO2 nanotubes”, J Appl Phys, vol. 112,2012, 104308.

[10] I. Manjubala, M. Sivakumar, S. Najma Nikkath,”Synthesis and characterisation of hydroxy/fluoroapatite solid solution’, J Mater Sci, vol. 36, 2001,pp 5481-5486.

[11] T.Shirai, H.Tsuchiya, T. Shimizu, K. Ohtani, Y. Zen, K.Tomita, “Prevention of pin tract infection with titanium-copper alloys”, J Biomed Mater Res, vol. 91B, 2009, 373–380

[12] F.Heidenau, W.Mittelmeier, R.Detsch, M.Haenle, F.Stenzel, G.Ziegler, H.Gollwitzer, "A novel antibacterial titania coating: metal ion toxicity and in vitro surface colonization. ",J Mater Sci Mater Med , vol. 16, 2005, pp. 883-888.

[13] J.Baker,S. Sitthisak, M. Sengupta, M. Johnson, R.K. Jayaswal, J.A. Morrissey, "Copper Stress Induces a Global Stress Response in Staphylococcus

aureus and Represses sae andagr Expression and Biofilm Formation", Appl.Environ. Microbiol., vol. 76, 2010, pp. 150-160.
[14]N. L Rosi , C.A. Mirkin, "Nanostructures in biodiagnostics. ", Chem. Rev., vol. 105, 2005, pp. 1547-1562.
[15]L.C. Ann, S. Mahmud, S. K. M.Bakhori, A. Sirelkhatim, D. Mohamad, H. Hasan, A. Seeni, R. A. Rahman, "Antibacterial responses of zinc oxide structures against Staphylococcus aureus, Pseudomonas aeruginosa and Streptococcus pyogenes", Ceram. Int., vol. 40, 2014, pp. 2993-3001.
[16] N. Patenge, K. Arndt, T. Eggert, C. Zietz, B. Kreikemeyer, R. Bader, B. Nebe, V. Stranak, R. Hippler, A. Podbielski, "Evaluation of antimicrobial effects of novel implant materials by testing the prevention of biofilm formation using a simple small scale medium-throughput growth inhibition assay. ", Biofouling., vol. 28, 2012, pp. 267-277.
[17] J.O. Noyce , H. Michels, C.W. Keevil , "Potential use of copper surfaces to reduce survival of epidemic meticillin-resistant Staphylococcus aureus in the healthcare environment", J Hosp Infect, vol. 63, 2006, pp. 289-297.
[18]G. Totea, D. Ionita, R. M. Katunar, S. Cere, I. Demetrescu,"Elaboration and characterization of the electrodeposited phosphates masses doped with various ions on stainless steel", Dig J Nanomater Bios, vol. 9, 2014, pp.575 – 584.
[19]Y. Song, S. Zhang, J. Li, C. Zhao, X. Zhang, "Electrodeposition of Ca–P coatings on biodegradable Mg alloy: in vitro biomineralization behavior", Acta Biomater, vol. 6, 2010, pp.1736–1742.
[20]L. Montazeri, J. Javadpour, M.A. Shokrgozar, S. Bonakdar, S. Javadian, "Hydrother-mal synthesis and characterization of hydroxyapatite and fluorhydroxyapatitenano-size powders", Biomed. Mater., vol.5, 2010, pp. 1–7.
[21] F. Freund, R.M. Knobel, "Distribution of fluorine in hydroxyapatite studied byinfrared spectroscopy", Dalton Trans, vol. 11,1977, pp. 1136–1140.
[22] M.A. El Mhammedi, M. Achak, M. Bakasse, A. Chtaini, "Physico-chemical characterization of electrochemical deposit of $Ca_{10}(PO_4)_6(OH)_2$ on copper surfaces" Appl. Surf. Sci., vol. 253, 2007, pp. 5925-5930.
[23] ASTM standard F2129, 2008, Standard test method for conducting cyclic potentiodynamic polarization measurements to determine the corrosion susceptibility of small implant device, ASTM, International, West Conshohocken, PA, 2001.
[24] B. Cao, Y. Zheng, T. Xi, C. Zhang, W. Song, K. Burugapalli,H. Yang,Y. Ma "Concentration-dependent cytotoxicity of copper ions on mouse fibroblasts in vitro: effects of copper ion release from TCu380A vs TCu220C intra-uterine devices", Biomed Microdevices, vol. 14, 2012,pp.709-720.
[25]U Lodemann , R.Einspanier ,F. Scharfen, H. Martens H,A. Bondzio"Effects of zinc on epithelial barrier properties and viability in a human and a porcine intestinal cell culture model", Toxicol In vitro, vol.27, 2013, pp.834-843.
[26] Totea, G., Ionita, D., Demetrescu, I., Mitache, M.M.: In vitro hemocompatibility and corrosion behavior of new Zr-binary alloys in whole human blood, Cent. Eur. J. Chem., 12, 796–803 (2014).
[27] Mariana Prodana, Daniela Ionita, Madalina Simoiu, Mihai Andrei, Antimicrobial effect of gentamicin incorporated in hydroxiapatite coating on 316L stainles steel, Analele Universităţii din Oradea-Fascicula Chimie, Vol. XXVI(27), 2020, p. 13-20.

Analele Universităţii din Oradea-Fascicula Chimie, Vol. XXVIII(28), 2021

INDIRECT SYNTHESIS OF KEGGIN POLYOXOMETALATES WITH TUNGSTEN AND VANADIUM ADDENDA

Anda Ioana Grațiela PETREHELE[1], Alexandrina FODOR[1], Claudia Mona MORGOVAN[1], Brenda PITTMAN[1]

[1] University of Oradea, Faculty of Informatic and Science, 1 Universiății, 410087, Oradea, Romania, e-mail: andapetrehele@yahoo.com

Abstract: *In this paper we aim to synthesize* $H_xPW_{12-x}V_xO_{40}$ *(x=1, 2, 3) indirectly, starting from lacunar Keggin compounds.* $H_4PW_{11}VO_{40}\cdot 10H_2O$ *was obtained from monolacunary* $K_7[PW_{11}O_{39}]$ *by the addition of vanadates under controlled conditions of pH and temperature, while* $H_6PW_9V_3O_{40}\cdot 16H_2O$ *was synthesized from the trilacunar species* $Na_9[HPW_9O_{34}]\cdot 11H_2O$ *in reaction with vanadate. For all prepared POM acids, the synthesis yields were very good and compounds with vanadium atoms were obtained in adjacent positions. Elementary analyzes, basicity determination, thermogravimetry, UV-VIS and FT-IR spectral data supported structure and composition HxPW12-xVxO40 (x = 1, 2, 3).* $H_xPW_{12-x}V_xO_{40}$ *(x=1, 2, 3) structure and composition.*

Key words: *Keggin, polyoxometalates, thermogravimetry, FT-IR, vanadium*

INTRODUCTION

POMs are compounds resulting from polycondensation reactions, in which oxyanions of transition metals from 5 and 6 groups are coordinated around metallic or non-metallic oxyanions. In the Keggin framework, each addenda atom M is octahedral surrounded by six oxygen atoms [1]. Of these, three octahedra are joined together by common edges that make M_3O_{13} type units. The four M_3O_{13} units are connected to each other by common corners [2]. In the maximum oxidation state M are generally molybdenum or tungsten atoms, but may be vanadium, niobium or tantalum atoms in the minority, in the maximum oxidation state [3].

Lacunary POMs are those structures that have been obtained by removing one or more MO_6 octahedra from a complete structure [4]. The absence of one or more octahedra in the structure gives the compounds an unsaturated character, which explains their great affinity for other atoms in high oxidation states as addenda (Mo, W, V, Nb), but also for metals cations in low oxidation states with which they form coordinative compounds [5].

The synthesis can be done directly from simply compounds of the component atoms or from another polyoxoanion already formed. Most polyoxoanion syntheses are performed in aqueous solution [6].

In this paper we aimed to synthesize three Keggin polyoxometalate (POM) compounds with ligands mixed addenda, tungsten and vanadium, starting from lacunary POM.

MATERIALS AND METHOD

All chemicals used were by high analytical purity. Distilled water used in all procedures. Conductometer and pH-meter analyses effectuated with a Multi 720 Inolab WTW series. Thermal stability analyses were performed in air on a Paulik-Erdely OD-103 derivatograph (20-800°C) at 5°C min^{-1}. FT-IR spectra were recorded in the 400-4000 cm^{-1} on a Biorad FTS 60A spectrophotometer using KBr pellets. UV-VIS spectra recorded in 190-1100 nm on T-60 UV-VIS model spectrophotometer.

$H_4PW_{11}VO_{40}\cdot 10H_2O$ synthesis

$H_4PW_{11}VO_{40}\cdot 10H_2O$ was obtained indirectly in several steps. In the first step, the acid $H_3PW_{12}O_{40}\cdot 4H_2O$ was obtained according to the literature [3]. It was transformed into the monolacunary species $K_7PW_{11}O_{39}$. A vanadate ion at pH 2 was added to monolacunary, and $H_4PW_{11}VO_{40}\cdot 10H_2O$ acid was isolated with ethyl ether in strong acid medium. The chemical reactions that formed the basis of this synthesis were:

$$12\,Na_2WO_4 + Na_2HPO_4 + 26HCl \rightarrow H_3[PW_{12}O_{40}] + 26NaCl + 12H_2O \quad (1)$$

$$H_3[PW_{12}O_{40}] + 9KHCO_3 \xrightarrow{pH\ 4,8} K_7[PW_{11}O_{39}] + K_2WO_4 + 6H_2O + 9CO_2 \quad (2)$$

$$K_7[PW_{11}O_{39}] + NaVO_3 + 8HCl \xrightarrow{pH\ 2} H_4[PVW_{11}O_{40}] + 7KCl + NaCl + 2H_2O \quad (3)$$

14.75 g (5 mmol) of $H_3[PW_{12}O_{40}]\cdot 4H_2O$ were dissolved in a minimum amount of water and 5% $KHCO_3$ was added under continuous stirring on a magnetic stirrer until pH 4.8 was reached. The $K_7[PW_{11}O_{39}]$ was filtered off and placed on a dry watch glass. In another Berzelius beaker 2 g (5 mmol) of $NaVO_3\cdot 4H_2O$ were dissolved in 30 ml of distilled water. 35% HCl was added dropwise to pH 4.8. Under stirring, small amounts of $K_7[PW_{11}O_{39}]$ began to be added and the pH of the reaction mixture was adjusted to pH 2 with 35% HCl. The mixture was put to react at 60 °C for 15 minutes. The heating was stopped and the pH was checked. If the pH was higher than 2, 35% HCl was added and the sample was left for another 15 minutes at 60 °C. The reaction mixture was cooled and then $H_3[PW_{12}O_{40}]\cdot 4H_2O$ was extracted with ethyl ether in HCl medium. The ether level was recovered from the heavy fraction of the separatory funnel and placed in rotavapor to remove the ether. The yield of intense yellow $H_4PW_{11}VO_{40}\cdot 10H_2O$ crystals was 73.08%.

$H_5PW_{10}V_2O_{40}\cdot 12H_2O$ synthesis

$H_5PW_{10}V_2O_{40}$ was obtained by adding two $NaVO_3$ units to the Keggin dilacunary unit, $K_7[PW_{10}O_{36}]\cdot 5H_2O$, according to literature data [3]. The method proposed by us ensures the vicinal position of the two vanadium atoms, which considerably can increase the catalytic properties of this compound [7, 8]. In the first stage, $K_7[PW_{10}O_{36}]\cdot 5H_2O$ dilacunary was synthesized, followed by the adding of two metavanadate units and $H_5PW_{10}V_2O_{40}\cdot 12H_2O$ formed. It was extracted in ethyl ether at acidic pH and after was separated by distillation. In this case the reactions were:

$$14H_3PO_4 + 10Na_2WO_4 + 7KCl \rightarrow K_7[PW_{10}O_{36}] + 7NaCl + 13NaH_2PO_4 + 8H_2O \quad (4)$$

$$K_7[PW_{10}O_{36}] + 2NaVO_3 + 8HCl \xrightarrow{pH\ 0,8} H_5[PV_2W_{10}O_{40}] + 7KCl + 2NaCl + 2H_2O \quad (5)$$

In 40 mL of distilled water 1.9 g (10 mmol) of $NaVO_3$·4H2O was dissolved at 70 °C. The solution was cooled to room temperature and 35% HCl was added to pH 0.8. In the yellow solution, under continuous stirring 14 g (5 mmol) of $K_7\,[PW_{10}O_{36}]\cdot 5H_2O$ were placed very slowly. The addition can take up to half an hour and during this time the pH is continuously adjusted with the concentrated HCl solution at pH 2. The solution obtained is filtered and the filtrate is extracted into ethyl ether in a separatory funnel. For a complete replacement of potassium cations with protons, the polyoxoanion solution obtained was passed over an ion-exchange resin regenerated with 0.1 N HCl. To better separate the ether beads, excess 35% HCl was added. The polyoxoanion ether was separated from the flask, and the ether was distilled off at 40 °C in a rotary evaporator on a water bath. The orange crystals were filtered and recrystallized from aqueous solution at 70 °C. $H_5PW_{10}V_2O_{40}\cdot 12H_2O$. The yield of the synthesis was 62.11%.

$H_6PW_9V_3O_{40}\cdot 16H_2O$ synthesis

As with the other two POM acids, the synthesis of this compound was performed in two steps. In the first stage, the trilacunary species, $Na_9[HPW_9O_{34}]\cdot 11H_2O$ at pH 9 was obtained, according to data from the literature [3]. $H_6PW_9V_3O_{40}\cdot 16H_2O$ was synthesized by the addition of three vanadate units to the trilacunary Keggin unit.

$$H_3PO_4 + 9Na_2WO_4 + 10H_3C-COOH \rightarrow Na_8[PW_9O_{34}] + 10H_3C-COONa + 6H_2O \quad (6)$$

$$Na_6[HPW_9O_{34}] + 3NaVO_3 + 9HCl \xrightarrow{pH\ 1,8} H_6PW_9V_3O_{40} + 9NaCl + 2H_2O \quad (7)$$

2.91 g (15 mmol) of $NaVO_3·4H_2O$ were dissolved in 40 ml of distilled water. The solution was brought to pH 5 with 35% HCl under continuous stirring and strict pH monitoring. 13.2 g (5 mmol) of α-Na8 $[HPW_9O_{34}]·11H_2O$ was added in small portions to the vanadium acid solution. The mixture was allowed to interact at room temperature under stirring overnight at room temperature. The pH was adjusted to 1.8 by the addition of 35% HCl. The polyacid obtained was separated from the reaction medium by extraction into ethyl ether in a separatory funnel. The ether was removed in a rotavapor under vacuo. The intense orange colour crystals of $H_6PW_9V_3O_{40}·16H_2O$ were separated and recrystallized from aqueous solution, so that the synthesis yield was 64.8%.

RESULTS AND DISCUSSIONS

Elemental analysis was performed for 5 g of each polyacid sample, degraded with 98% H_2SO_4 at boiling for 30 minutes. The obtained solution was filtered and divided in two. The first part of the solution was treated with 8-hydroxyquinoline and after the reaction the tungsten and vanadium ions precipitated together. The total amount of vanadium and tungsten was determined gravimetrically [7]. The filtrate was used for photocolorimetric determination of phosphorus with the T60 spectrophotometer [8]. The other half of the initial solution was used to determine vanadium by reduction and complexation with EDTA [9]. In this situation, only tungsten was precipitated and it was determined gravimetrically. The results of the elemental analysis performed for the three Keggin polyacids are recorded in Tab. 1. The elemental analysis confirmed molar ratios P:V:W characteristic for synthesized compounds.

Table 1. Elemental analyses of $H_xPW_{12-x}V_xO_{40}$ (x=1, 2, 3)

Sample mass (mg)	Molar mass	Element	Experimental data mg (mmol)	Theoretical data mg (mmol)
$H_4PW_{11}VO_{40}·10H_2O$ (4863.1)	2928.31	P V W	51 (1.65) 80 (1.57) 3350 (18.23)	51.41 (1.66) 84.56 (1.66) 3356.5 (18.26)
	Molar rate	P:V:W	1:1:11	1:1:11
$H_5PW_{10}V_2O_{40}·12H_2O$ (5.0177)	2832.45	P V W	54 (1.74) 180 (3.53) 3250 (17.68)	54.82 (1.77) 180.33 (3.54) 3254 (17.71)
	Molar rate	P:V:W	1:2:10	1:2:10
$H_6PW_9V_3O_{40}·16H_2O$ (4.9805)	2772,62	P V W	55 (1.78) 270 (5,3) 2970 (16.16)	55.75 (1.8) 275.08 (5.4) 2978.2 (16,2)
	Molar rate	P:V:W	1:3:9	1:3:9

In Tab. 2 the data obtained from the thermogravimetric analysis of the three diagrams TG, DTG and DTA for polyoxometalates $H_4PW_{11}VO_{40}·10H_2O$, $H_5PW_{10}V_2O_{40}·12H_2O$ and $H_6PW_9V_3O_{40}·16H_2O$ were recorded [10]. In the TG curve a mass loss can be observed in the thermal range 20-200 °C, attributed to the hydration water molecules. The weight loss was 6.15%, which corresponded to 10 molecules of hydration water for $H_4PW_{11}VO_{40}·10H_2O$; of 8.69% for $H_5PW_{10}V_2O_{40}·12H_2O$, which corresponds to 12 water molecules and 10.38 for $H_6PW_9V_3O_{40}·16H_2O$ corresponding to 16 water molecules. In the DTA curve, the loss of zeolitic water is marked by an intense endothermic process at over 110 °C for all three compounds. The exothermic process detected at temperatures above 340 °C was associated with the destruction of the structural framework of POM. According to the obtained data it results that the most stable species was found $H_4PW_{11}VO_{40}·10H_2O$ with one vanadium atom, and the most unstable was $H_6PW_9V_3O_{40}·16H_2O$ with three substituted vanadium atoms. In other words, the stability of synthesized POM with mixed addenda decreases with increasing of vanadium atoms number. Endothermic processes at temperatures above 700 °C were caused by the decomposition of oxyanions, the formation of oxides of component atoms and by their possible structural changes.

Table 2: Thermogravimetry analyses of $H_xPW_{12-x}V_xO_{40}$ (x=1, 2, 3)

	DTA (° C)		DTG (° C)	TG	
				mass loss (%)	H_2O molecules
$H_4PW_{11}VO_{40}\cdot10H_2O$	endotherm exotherm endotherm	125 380 723 764 800	122 372	6.15 %	10
$H_5PW_{10}V_2O_{40}\cdot12H_2O$	endotherm exotherm endotherm	112 365 710 743 790	105 340	8.69 %	12
$H_6PW_9V_3O_{40}\cdot16H_2O$	endotherm exotherm endotherm	107 340 700 725 770	103,5 325	10.38 %	16

The basicity was determined by potentiometric titration with a Multi 720 multimeter. The method consisted in titrating of 0.01 M $H_xPW_{12-x}V_xO_{40}$ (x = 1, 2, 3) solutions with a 0.1 M NaOH solution. For 10 mL $H_4PW_{11}VO_{40}$ were consumed 4 mL NaOH, corresponding to a molar rate NaOH:$H_4PW_{11}VO_{40}$ equal with 4, in concordance with presence of four protons in this polyacid structure. Similar situations were found for both $H_5PW_{10}V_2O_{40}$ and $H_6PW_9V_3O_{40}$where five and six NaOH moles were necessary to neutralize the acid character of their protons, confirming to five and six their basicity [1,7].

The FT-IR spectrum of $H_5PW_{10}V_2O_{40}\cdot12H_2O$ was recorded in Fig. 1. The values of the maximum absorbances obtained for the three studied compounds are noted in Table 3. In the spectrum we could see the presence of a wide and intense band at over 3600 cm^{-1} attributed to the asymmetric vibration of OH group, ν_{as}(OH), due to water molecules crystallization [11]. The band of medium intensity δ(OH) around 1620cm^{-1} was caused by the deformation in the plane vibration of H-O-H bonds in the water crystallization molecules [4]. Signals recorded in 1100-1000 cm^{-1} were attributed to the asymmetric stretching vibration ν_{as}(P-O$_i$), where Oi realized the link between phosphorus and addenda atoms (W and V). For $H_4PW_{11}VO_{40}\cdot10H_2O$ an intense band was found at 1103 cm^{-1} with and one less intense at 1082 cm^{-1} due to the asymmetry created by the presence of vanadium atoms. For $H_5PW_{10}V_2O_{40}\cdot12H_2O$ there were three signals due to the coordination of two vanadium atoms. Triple splitting indicates an increase of the asymmetry degree within the polyoxoanion edifice, and the shift to lower frequencies was due to increase of the molecular instability caused by the presence of two vanadium atoms in the framework [5]. In the case of $H_6PW_9V_3O_{40}\cdot16H_2O$ two signals were shifted to lower frequencies pointing even lower structural stability. The vibration at 1089 cm^{-1} was significantly more intense than at 1059 cm^{-1} and was attributed to the P-Oi oxygen bonds with tungsten atoms, while the less intense vibration was due the linkage to vanadium atoms. The transition from three vibrations for divanadate complex to two vibrations in trivanadate confirmed that the three vanadium atoms were in neighboring positions, and the degree of symmetry of the three-vanadium compound was higher. The very intense band from 990-960 cm^{-1} was given by the asymmetric vibrations ν_{as} (M-O$_t$) where Ot was a terminal oxygen atom attached to each addenda atom. For the M-O$_c$-M bond, (O$_c$ was a common corner oxygen atom between two addenda atoms) an intense band was obtained at 900-870 cm^{-1}, and for M-O$_e$-M bond, (O$_e$ was common edge oxygen atom between two addenda) an intense band in 800-790 cm^{-1} was obtained. This second band showed a shoulder for all three compounds emphasizing the existence of two types of addenda atoms

.

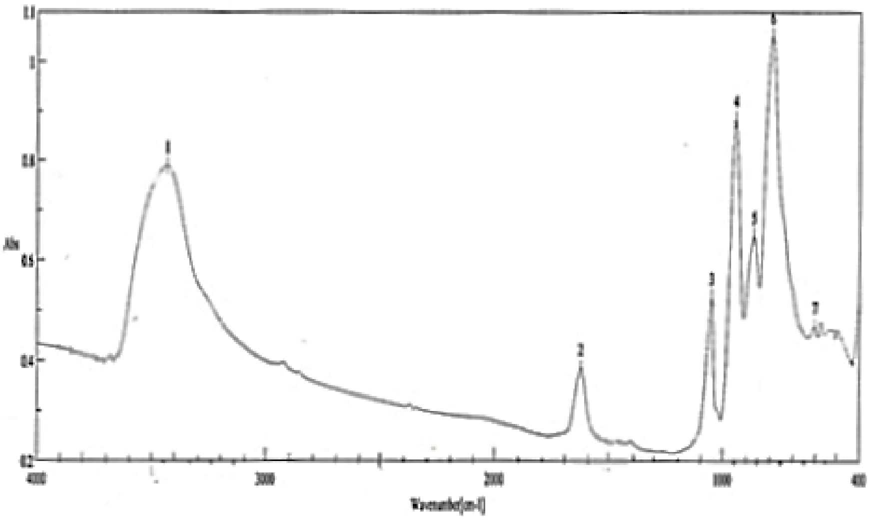

Figure 1. FT-IR spectrum of $H_5PW_{10}V_2O_{40}{\cdot}12H_2O$

Table 3. FT-IR data of $H_xPW_{12-x}V_xO_{40}$ (x=1, 2, 3)

Compound	$\nu_{asymetric}$ (P-O$_i$) cm^{-1}	$\nu_{symetric}$ (Mo-O$_t$) cm^{-1}	$\nu_{asymetric}$ (Mo-O$_c$-Mo) cm^{-1}	$\nu_{asymetric}$ (Mo-O$_e$-Mo) cm^{-1}	$\nu_{asymetric}$ (OH) cm^{-1}	$\delta_{asymetric}$ (OH) cm^{-1}
$H_4PW_{11}VO_{40}{\cdot}10H_2O$	1103 1082	990	885	789 sh	3649	1618
$H_5PW_{10}V_2O_{40}{\cdot}12H_2O$	1100 1079 1062	966	898	792 sh	3650	1637
$H_6PW_9V_3O_{40}{\cdot}16H_2O$	1089 1059	960	871	796 sh	3741 3481	1625

The electronic spectra were plotted in aqueous solution in the concentration range 0.01–10 mM and were characteristic for POM compounds with Keggin complete structure. In the UV-VIS spectrum of $H_5PW_{10}V_2O_{40}{\cdot}12H_2O$ (Fig. 2) two characteristic transfer bands were observed, ν_1 due to the electronic transition d_π-p_π-d_π from M-O$_{c,e}$-M bonds, which occurs at 247 nm and ν_2 due to the electronic transition d_π-p_π from the M = O$_t$ bonds, which occurs at 201.5 nm [5, 12].

In Table 4 the values of maximum absorbance obtained for all three polyacids studied are pointed in. It could be observed that as the number of vanadium atoms inside the polyoxoanion edifice increased, the maximum band corresponding to the electronic transition dπ-pπ from the M=O$_t$ bonds was moved to shorter wavelengths, while the charge transfer band , ν1 due to the electronic transition dπ-pπ-dπ from the M-O$_{c,e}$-M bonds were moved to longer wavelengths, into the visible range [1].

This second shift was also the result of in the intensification of the POM color as the number of vanadium atoms increased inside their structure [12].

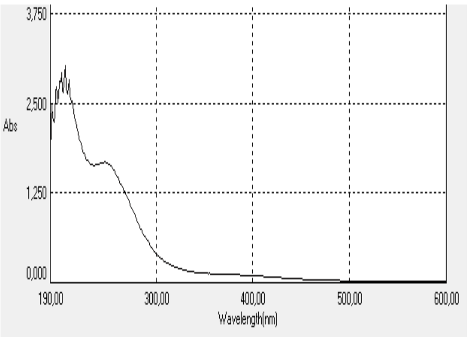

Fig. 2. UV-VIS spectrum of $H_5PW_{10}V_2O_{40}{\cdot}12H_2O$

Table 4. UV-VIS date of $H_xPW_{12-x}V_xO_{40}$ (x=1, 2, 3)

Compounds	Electronic transition bands ν/λ (cm^{-1}/nm)	
	ν_1 (M-$O_{c,e}$-M)	ν_2 (M=O_t)
$H_4PW_{11}VO_{40}\cdot 10 H_2O$	38310/261	50000/200
$H_5PW_{10}V_2O_{40}\cdot 12 H_2O$	40490/247	49630/201,5
$H_6PW_9V_3O_{40}\cdot 16 H_2O$	42010/238	49260/203

CONCLUSIONS

Despite the fact that the indirect method is a more laborious one requiring a longer synthesis time with careful attention to all stages, it has the advantage of leading to obtaining POM with a high degree of purity, with high yields. In the case of acids with several vanadium atoms, isomers would be obtained in which they occupy the adjacent positions, which makes the utility of these compounds much more interesting from a practical point of view.

REFERENCES

[1] Pope, M.T. (1983). Poly and Isopoly Oxometalates, Ed. Springer-Verlag, Berlin, Heidelberg, New-York, Tokyo.

[2] Souchay, P. (1969). Ions Mineraux Condenses, Ed. Masson, Paris.

[3] Marcu, Gh. (1984). Chimia compușilor coordinativi, Ed. Acad. R.S.R., București.

[4] Marcu, Gh., Rusu, M. (1997). Chimia polioxometalaților, Ed. Tehnică, București.

[5] Pope, M. T., Muller, A (1991). Angew. Chem. Int., Ed. Engl., 30, pp. 34-48.

[6] Neumann, R. (2007). Polyoxometalate Complexes in Organic Oxidation Chemistry, in Progress in Inorganic Chemistry, Ed. K. D. Karlin John Wiley & Sons, Inc., Hoboken, NJ, USA.

[7] Domaille, P. J., Hervéa, G., Téazéa, A. (2007). Vanadium(V) Substituted Dodecatungstophosphates, in Inorganic Syntheses**,** Ed. John Wiley & Sons, Inc.: Hoboken, NJ, USA.

[8] Cavaleiro, A. M. V., Pedrosa de Jesus, J. D., Nogueira, H. I. S. (1999). Metal Clusters in Chemistry , Ed. P. Braunstein, L. A. Oro, P. R. Raithby, VCH, pp. 444-458.

[9] Tadaharu U., Masashi K., Masashi H. (2003), Spectroscopic and voltammetric studies on the formation of Keggintype V(V)-substituted tungstoarsenate(V) and -phosphate(V) complexes in aqueous and aqueous-organic solutions, Inorg. Chim. Acta 344, pp. 77-84

[10] Kenji N., Yoshitaka S., Yoshiteru Y., Takeshi H. (2001), Synthesis and spectroscopic characterization of a Keggin 1,4,9-trivanadium-substituted polyoxotungstate-supported Cp*Rh2 complex, [(Cp*Rh)(-1,4,9-PW9V3O40)]$^{4-}$, J. Chem. Soc., Dalton Trans., pp. 52–56

[11] Huang W., Todaro L., Yap G. P. A., Beer R., Francesconi L. C., Polenova T. (2004), ^{51}V Magic Angle Spinning NMR Spectroscopy of Keggin Anions [PVnW12-nO40]$^{(3+n)-}$: Effect of Countercation and Vanadium Substitution on Fine Structure Constants, J. Am. Chem. Soc., Vol. 126, pp. 11564-11573

[12] Lever, A.B.P. (1984). Inorganic Electronic Spectroscopy, Ed. Elsevier, New York

Analele Universităţii din Oradea-Fascicula Chimie, Vol. XXVIII(28), 2021

SHORT REVIEW ON FREE SOFTWARE FOR CHEMICAL MOLECULAR STRUCTURES

Petru Gabriel BADEA[1], Gabriela Elena BADEA[2]
[1.] student- Informatics, Faculty of Informatics and Science, University of Oradea, badea.petrugabriel@student.uoradea.ro
[2] Department of Chemistry, Faculty of Informatics and Science, University of Oradea, gbadea@uoradea.ro

Abstract. *The development of information technology, smart technologies and the growing demand for better visibility has led to the need to create applications in the field of chemistry, which should include primarily a drawing editor for the creation of molecular structures (like 2D, 3D), and their correlation with categories or classes of substances, respectively the creation of databases with physico-chemical properties, correlated with the structure or other instruments, such as the molecular mass calculation. This article is a short review of free software applications available on the Internet, meaning that these type of aplications could become important resources not only for chemists, but also for any scientific and engineering researchers.*

Key words: software, drawing editor, chemistry,chemical molecular structure

INTRODUCTION

The application of computer science in the study of sciences, such as chemistry, biology has led to the emergence of new directions for the development of software applications, such as: computational chemistry, chemoinformatics [1], chemical mathematics, bioinformatics, molecular modeling [1,2].

Computational chemistry aims to develop mathematical models, which simulate chemical systems, to calculate or predict physical and chemical properties. To run simulations in real time, they are correlated with the power of computers: the number of floating point operations per second (Flops)or the memory capacity. If the theoretical support is already known since the middle of the twentieth century, the development became possible only with the appearence of sufficiently powerful hardware systems [2]. Chemoinformatics aims to use techniques such as storing information about physico-chemical properties, so the creation of computer databases [1].

The huge amounts of chemistry experimental data determined in the last decades , the chemoinformatics applies techniques development from artificial intelligence, pattern recognition and machine learning. Elucidation of chemical structure and its correlation with the substance properties are key tasks in computational chemistry, for learning, teaching or reaserch [1-16].

For example , the NMR spectra related to molecule structural properties have been approuched using Bayesian networks [3]. The the of benzenoids hydrocarbons , their structure and related chemical properties by Choco Solver modelling could allow generate specimens by constraint programming Modeling Graph variables[4]. New concept of chemical modeling involve an semi-empirism Polymorphic trees Generalized chromophores Cartesius fort library , for " efficient parallelization and more efficient usage of the HPC"[5]. Experimentally and theoretically data regarding molecular structure containg conformations involving torsions around O – O and S – S bonds ilustrated by the mean of a screen , made a conection " *between the classical kinematic mechanism – the four-bar linkage – and the basic ingredient of quantum angular momentum theory – the 6j symbol.* ""[6]. Other authors presents "*Dimmol (acronym for Distributed Immersive Multi-platform Molecular visualization), a scientific visualization application based on UnityMol, developed with the Unity game engine, and that uses the Unity Cluster Package to enable distributed and immersive visualization of molecular structures across multiple device of different types, with support to Google VR, molecular trajectory files, and master-host-*

slave rendering"[7]. An intelligent CAI system for chemistry was developed based on automated reasoning using chemistry knowledge. This system has an unique style of the interface and could assist students and teachers The automated reasoning is also opened to " *a new approach to the information storage and management of the ICAI system for sciences*"[8]. An algorithms of heuristic nature to compute standardised 2*D* structure drawings was proposed by c Chen [9] for evaluating the molecular structures, by comparing their 2D structure drawings. This is a usual strategy used in strategy when drug design and pharmacophore identification. G.Valiente [12] describe alogorithms based on an intuitive aproach, using structured pseudocode, giving extensive explanaition on the algorithmic techniques.

OPEN SOURCE AND COMMERCIAL CHEMISTRY SOFTWARE APPLICATIONS

With the development of communications technology, especially in smart technologies, the image, the visual content has become very important for visibility in general, but also in those areas that operate with theory related to the intimate structure of matter, with those elements that can not be seen, but for which researchers especially in the fields of chemistry and physics have created 2D or 3D models to make knowledge more accessible.

To keep up with this demand for visual content, software applications have begun to grow and become more complex. Software applications for editing chemical formulas and structures can be supplemented with a number of useful tools such as: molecular weight calculation, correlation of a structure with the physical and chemical properties of the substance or creation of databases with substances, structured by different categories.

Table 1 partially shows a number of such applications of computational chemistry, as listed at https://koaha.org/wiki/Listory_of_software_of_computational_chemics [2]. The table also allows access to various programs on the link, which is obviously an advantage. The programs presented are either open source or commercial programs with one or more modules. Some applications support . "periodic systems (crystals, 3d; surfaces, 2d; polymers, 1d and molecules, 0d; 3d periodicity software always allows the simulation of smaller dimensional systems. Most of these applications include Hartree-Fock (HF) and some post-Hartree-Fock methods, functional density theory (DFT), molecular mechanics and semi-empirical methods"[2]

DISCUSSIONS ABOUT SOME FREE CHEMISTRY SOFTWARE

Here are brief presentions of some free chemistry software [14-16]

ACDLabs

The **ACDLabs** program [14] includes two modules **ACD / ChemSketch** and **ACD / Labs.**

ACD/ChemSketch Freeware Module is a "*drawing package that allows you to draw chemical structures including organics, organometallics, polymers, and Markush structures. It also includes features such as calculation of molecular properties (e.g., molecular weight, density, molar refractivity etc.), 2D and 3D structure cleaning and viewing, functionality for naming structures (fewer than 50 atoms and 3 rings), and prediction of logP. The freeware version of ChemSketch does not include all of the functionality of the commercial version* " [14].

ACD/Labs software is a teaching tool, using " *key chemistry concepts to high school, undergraduate, and graduate chemistry students. In addition, students benefit from exposure in the learning environment to the same tools they will encounter in the workforce. ACD/ChemSketch Freeware is a drawing package that allows you to draw chemical structures including organics, organometallics, polymers, and Markush structures. It also includes features such as calculation of molecular properties (e.g., molecular weight, density, molar refractivity etc.), 2D and 3D structure cleaning and viewing, functionality for naming structures (fewer than 50 atoms and 3 rings), and prediction of logP*. " [14] This aplication could be very usefull for qualifying academic institutions to make available to their students and faculty.

Table 1. List of some computational chemistry software [2, 17].

Software	**Licence**[†]	Base	**Periodical Systems** [‡]	**Molecular Mechanics**	**Semi-empiric methods**	**HF**	**Post-HF**	**DFT**
ABINIT	GPL	PW	3d	S.	No.	No.	No.	S.
ACES II	acad.	GTO	No.	No.	No.	S.	S.	S.
ADF	com.	STO	any	S.	S [4]	S.	No.	S.
Atomistix ToolKit	com.	NAO	3d	S.	No.	No.	No.	S.
CADPAC	acad.	GTO	No.	No.	No.	S.	S.	S.
CASTEP	acad. (UK) / com.	PW	3d	S.	No.	S [5]	No.	S.
CFOUR	acad.	GTO	No.	No.	No.	S.	S.	No.
CP2K	GPL	GTO / PW hibrid	any	S.	S.	S.	No.	S.
CPMD	acad.	PW	any	S.	No.	S.	No.	S.
CRISTAL	acad. (UK) / com.	GTO	any	S.	No.	S.	No.	S.
YESLTON	acad.	GTO	No.	No.	No.	S.	S.	S.
DFTB +	acad./com.	NAO	any	S.	S.	No.	No.	No.
DIRAC	acad.	GTO	No.	No.	No.	S.	S.	S.
FreeON	GPL	GTO	any	S.	No.	S.	S.	S.
GAMESS (Marea Britanie)	acad. (UK) / com.	GTO	No.	No.	S.	S.	S.	S.
GAMESS (SUA)	acad.	GTO	No.	S [2]	S.	S.	S.	S.
GAUSSIAN	com.	GTO	any	S.	S.	S.	S.	Yes
GPAW	GPL	grilă / NAO	any	S.	?	S [5]	No.	S.
JAGUAR	com.	GTO	?	S.	No.	S.	S.	S.
MOLCAS	com.	GTO	No.	S.	S.	S.	S.	S.
MOLPRO	com.	GTO	?	No.	No.	S.	S.	S.
MOPAC	acad. / com.	?	?	?	S.	No.	No.	No.
MPQC	LGPL	GTO	No.	No.	No.	S.	S.	S.
NWChem	acad.	?	?	S.	No.	S.	S.	S.
ONETEP	acad.(UK) / com.	PW	any	S.	No.	S [5]	No.	S.
OpenAtom	acad.	DVR	?	S.	No.	No.	No.	S.
OpenMX	GPL	NAO	3d	S.	No.	No.	No.	S.
PLATON	acad.	NAO	any	S.	No.	No.	No.	S.
PSI	GPL	GTO	No.	No.	No.	S.	S.	No.
PWscf [6]	GPL	PW	3d	No.	No.	S.	No.	S.
PyQuante	BSD	GTO	No.	No.	S.	S.	S.	S.
Q-Chem	com.	GTO	No.	S.	S.	S.	S.	S.
ESPRESSO cuantic	GPL	PW	3d	No.	No.	Yes	No.	Yes
SPARTAN 06	com.	GTO	?	Yes	Yes	Yes	Yes	Yes
TURBOMOLI	com.	GTO	?	Yes	No.	Yes	Yes	Yes
WIEN2k	com.	FP- (L) APW + lo	3d	Yes	No.	Yes	No.	Yes

Notations [2]:

[†] "acad.": academic license (free), "com.": commercial license

[‡] Support for periodic systems (crystals, 3d; surfaces, 2d; polymers, 1d and molecules, 0d): 3d periodic software always allows the simulation of smaller dimensional systems.

[2] Through the TINKER interface

[3] Through Ascalaph

[4] Through the MOPAC interface

[5] Using the exact DFT exchange theory

[6] Distributed with Quantum ESPRESSO

[7] MPQC integrated web services.

ChemDoodle2D

ChemDoodle 2D and could be found at the adress: https://www.chemdoodle.com/ and is a program containing a lot of chemistry features, with highest quality graphics, as following: 2D graphics, drawing, IUPAC Naming, cheminformatics, reactions, spectroscopy, vector art.[15]

Build a molecule

Build a Molecule is a free Windows apllication , creating a Chemistry simulation environment, where could found or simulate 3D molecular structure and a data base of different chemical substances.[16]

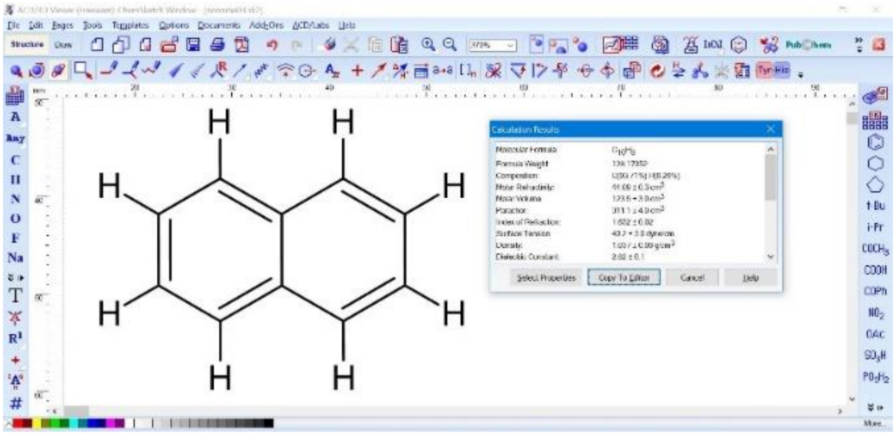

Calculation Results

Molecular Formula	$C_{10}H_8$
Formula Weight	128.17052
Composition:	C(93.71%) H(6.29%)
Molar Refractivity:	44.09 ± 0.3 cm^3
Molar Volume:	123.5 ± 3.0 cm^3
Parachor:	311.1 ± 4.0 cm^3
Index of Refraction:	1.602 ± 0.02
Surface Tension:	40.7 ± 3.0 dyne/cm
Density:	1.037 ± 0.06 g/cm^3
Dielectric Constant:	2.82 ± 0.1

Figure 1. Capture from freeware ACD/ChemSketch.
https://www.acdlabs.com/resources/freeware/chemsketch/index.php [14]

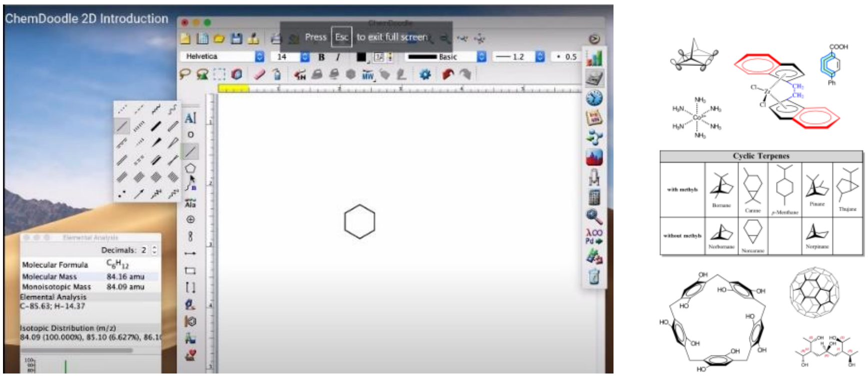

Decimals: 2

Molecular Formula C_6H_{12}
Molecular Mass 84.16 amu
Monoisotopic Mass 84.09 amu
Elemental Analysis
C-85.63; H-14.37

Isotopic Distribution (m/z)
84.09 (100.000%), 85.10 (6.627%), 86.1

Figure 2. Captures from freeware ACD/ChemSketch.[15]
https://www.chemdoodle.com/

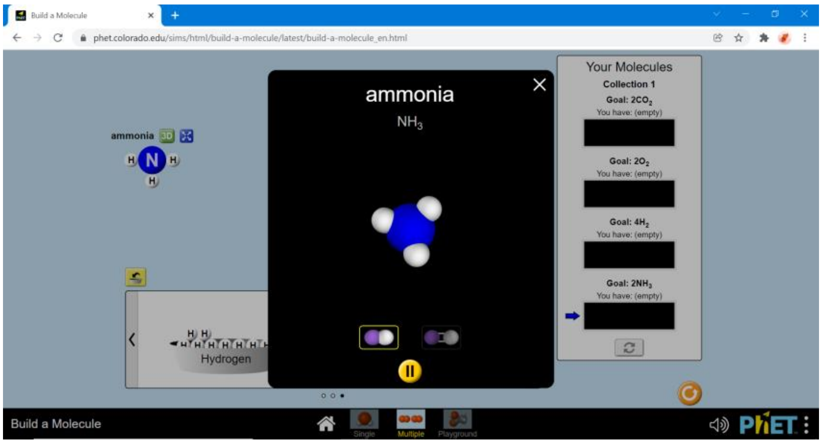

ammonia
NH_3

Your Molecules
Collection 1
Goal: $2CO_2$
You have: (empty)
Goal: $2O_2$
You have: (empty)
Goal: $4H_2$
You have: (empty)
Goal: $2NH_3$
You have: (empty)

*Figure 3. Captures from freeware **Build a molecule** [16]*
https://phet.colorado.edu/sims/html/build-a-molecule/latest/build-a-molecule_en.html

CONCLUSIONS

Obviously, software applications for chemistry cover a wide range of concerns, from images, graphs, databases, numerical calculations and simulations.

This paper cannot be an exhaustive presentation, it only comes to highlight the existence and importance of informatics in the study of chemistry and in particular of computational chemistry, as a working tool.

REFERENCES

[1] https://ro.wikipedia.org/wiki/Chemoinformatic%C4%83
[2] https://koaha.org/wiki/Chimica_computazionale
[3].Michaela Hohenner , Sven Wachsmuth, Gerhard Sagerer, Modelling Expertise for Structure Elucidation in Organic Chemistry Using Bayesian Networks, International Conference on Innovative Techniques and Applications of Artificial Intelligence, SGAI 2004: Applications and Innovations in Intelligent Systems XII pp 251-264.
[4]Yannick Carissan, Denis Hagebaum-Reignier, Nicolas Prcovic, Cyril Terrioux, Adrien Varet, Using Constraint Programming to Generate Benzenoid Structures in Theoretical Chemistry, International Conference on Principles and Practice of Constraint Programming, CP 2020: Principles and Practice of Constraint Programming, pp 690-706.
[5]Andrei L. Tchougréeff , Cartesius fort - object fortran Library for Chemistry and Materials Science, International Conference on Computational Science and Its Applications, ICCSA 2019: Computational Science and Its Applications – ICCSA 2019 pp 639-651.
[6] Vincenzo Aquilanti, Concetta Caglioti, Andrea Lombardi, Glauciete S. Maciel, Federico Palazzetti, Screens for Displaying Chirality Changing Mechanisms of a Series of Peroxides and Persulfides from Conformational Structures Computed by Quantum Chemistry, International Conference on Computational Science and Its Applications, ICCSA 2017: Computational Science and Its Applications – ICCSA 2017 pp 354-368.
[7] Luiz Soares dos Santos Baglie, Mário Popolin Neto, Marcelo de Paiva Guimarães, José Remo Ferreira Brega, Distributed, Immersive and Multi-platform Molecular Visualization for Chemistry Learning, International Conference on Computational Science and Its Applications, ICCSA 2017: Computational Science and Its Applications – ICCSA 2017, pp 569-584.
[8] Wang Xiaojing , Zhang Jingzhong , The intelligent CAI system for chemistry based on automated reasoning, *Journal of Computer Science and Technology*, volume 14,pages495–509 ,1999.
[9] J. D. Boissonnat, F. Cazals, J. Flötotto, 2*D*-Structure Drawings of Similar Molecules, International Symposium on Graph Drawing, GD 2000: Graph Drawing pp 115-126
[10]J.Y. Ramel, N. Vincent , H. Emptoz , A structural representation for understanding line-drawing images, *International Journal on Document Analysis and Recognition* volume 3, pages58–66 (2000).
[11]Chaomei Chen, Spatial Layout and Graph Drawing Algorithms, Information Visualisation and Virtual Environments, pp 61-91, 1999.
[12] Gabriel Valiente, Algorithms on Trees and Graphs With Python Code, Texts in *Computer Science* book series , Springer, 2nd ed., 2021.

[13]Joshua Ho, Seok-Hee Hong, Drawing Clustered Graphs in Three Dimensions, International Symposium on Graph Drawing, GD 2005:Graph Drawing, pp 492-502, Part of the *Lecture Notes in Computer Science,* book series (LNCS, volume 3843).
[14]https://www.acdlabs.com/resources/freeware/chemsketch/index.php
[15]https://www.chemdoodle.com/
[16]https://phet.colorado.edu/sims/html/build-a-molecule/latest/build-a-molecule_en.html
[17] David Young,*Computational Chemistry: A Practical Guide for Aplicating Techniques to Real World Problems*, New York, John Wiley & Sons, 2001, pp. 322–359, ISBN 0-471-33368-9.

Analele Universităţii din Oradea-Fascicula Chimie, Vol. XXVIII(28), 2021

TOXICITY ANALYSIS OF ANIONIC AND CATIONIC DETERGENTS

Alexandra DAROCZI[1], Mioara SEBEŞAN[2], Oana Delia STĂNĂŞEL[2],
Gabriela Elena BADEA[2], Radu SEBEŞAN[3], Sorin HODIŞAN[2]

[1] student master CSA anul II, Universitatea Oradea,
Facultatea de Informatică şi Ştiinţe
[2]Universitatea din Oradea, Facultatea de Informatică şi Ştiinţe,
[3]University of Oradea, Faculty of Electrical Engineering and Information Technology,

Abstract. *In this paper we will analyze the activity of some surfactants, which can be toxic in certain detergents. We will analyze the anionic and cationic surfactants by different identification methods using indicators, but we will also quantitatively determine the concentrations of anionic and cationic detergents with the help of the UV-VIS spectrophotometer.*

Keywords*: surfactants, cationic detergents, anionic detergents, UV-VIS spectrophotometer*

INTRODUCTION

The detergents themselves are complex salts of some synthesized acids. The detergent molecule has a lipophilic and hydrophobic extremity. They have the property of fixing themselves to a fat molecule, but not to water molecules. In the composition of the molecule there is also a nonpolar hydrocarbon, lipophobic and hydrophilic chain, that is, it does not fix on fats, but it is fixed on water molecules. The hydrophilic extremities are miscible with water, the lipophilic ones are fixed on the fat molecules, so the detergent molecules are fixed at the interface between water and fat, detaching the fats from the textile support.

In the compositions of detergent molecules, two important categories of components are distinguished:
-basic components: surfactants, abrasives, acids, alkalis, bleaches and enzymes
-secondary components: excipients, water softeners, perfumes, antipollutants, special polymers, etc. [1]

In this work we will study the toxicity of detergents, more precisely the toxicological action of some surfactants. The most famous surfactants on the market and the most often used to obtain detergents are: betaines, amine oxides, alkyl polyglucosides, alkyl sulfate, ethoxylate alcohols, alkyl ethoxylate phenol, ether sulfate, alkyl benzene sulfonate.

Unfortunately, some synthetic surfactants that are manufactured in large quantities, such as alkyl benzene sodium sulfonate, are resistant to biodegradation and resist and foam in treatment plants and even in rivers, wherever they occur in large quantities. These non-degradable surfactants cannot be easily removed from surface waters.

The biodegradability of surfactants is a particular problem that is directly related to the increase in surfactant consumption, which also causes the increase of the concentration of surfactants in wastewater.

In the manufacture and use of surfactants, account must be taken of their effects on man and the environment.

MATERIALS AND METHODS

Spectrometric methods are a particularly broad and diverse category of analytical methods, its applications appearing in different fields such as chemical, pharmaceutical, medicine, agriculture, food quality control, etc. Spectrometry includes a set of methods based on the use of electromagnetic radiation of all wavelengths which, when passing through a substance, causes absorption, emission, diffusion phenomena, which can be measured with specific apparatus. Electromagmetic radiation is represented by electric and magnetic fields that propagate linearly and at a constant speed.

The totality of electromagnetic frequencies constitutes the electromagnetic spectrum. It covers a very large area, from values of 103 Hz, up to 1019 Hz. The electromagnetic spectrum is divided into spectral domains, depending on the interaction of radiation with the material, but also according to the type of transitions that take place in the molecules. [6]

The property of substances to selectively absorb electromagnetic radiation is the basis of absorption spectrophotometry and is used for identification, determination of purity and dosing.

Absorption spectrophotometry includes the methods of analysis based on the modification of the intensity of the electromagnetic radiation when passing through a solution, due to the absorption of a certain amount of the radiation energy, at a certain wavelength, by the solution to be investigated. Thus, absorption spectra are formed. The amount of energy absorbed is depending on the structure and number of molecules and atoms of the substance with which the radiation beam interacts.

Depending on the spectral domains in which the absorption of light takes place, the following are distinguished:

-ultraviolet spectrophotometry (100-200 nm-vacuum UV, 200-380 nm-uv near)

-spectrophotometry in visible (380-780 nm)

-infrared spectrophotometry (over 800 nm).

The molecular absorption spectrometry in UV-VIS is based on the absorption by molecules of light radiation from the range of 200-780 nm. This operation results in the passage of electrons from the fundamental state to the excited state, with electronic transitions taking place. In spectrophotometry, sizes such as P0= the incident radiant power, Pt= the transmitted radiant power, are used as the energy of the radiation transported by an incident luminous flux, respectively transmitted, on an area of 1 cm2 in a second.

Qualitative analysis is based on the knowledge of the value of the wavelength at which the sample to be analyzed absorbs. The calibration/calibration curve is the graphical representation of the absorbance as a function of concentration, using for quantitative determinations.

Analysis of cationic detergents

Principle: the quaternary caation from the cationic detergent forms, in alkaline medium, with the methyl orange anionic dye (H3C)2N-C6H4-N=N-C6H4-SO3Na colored compounds, extractable in chloroform. [7]

***Reagents*:** cationic detergent, 0,15 % methyl orange solution, 10 % sodium hydroxide solution, chloroform and 2N hydrochloric acid

Materials: Erlenmayer glasses, volumetric flasks, cylinder, funnel, technical balance

Working method: Measure the extinctions to the spectrophotometer at 508 nm in a 1 cm vat against the reagent tell-tale. The extinction value of the sample is related to the standard curve, obtaining the concentration C in µg of cationic detergent in the sample.

Calculation:

Mg cationic detergent/100 ml analyzed product

Solutions of different concentrations have been prepared:

C1- weighed 0.001 g detergent, placed in a 1 l volumetric flask and supplemented with distilled water to the mark

C2- weighed 0.01 g detergent, placed in a 1 l volumetric flask and supplemented with distilled water to the mark

C3- weighed 0.05 g detergent, placed in a 1 l volumetric flask and supplemented with distilled water to the mark

C4- x g detergent, it was placed in a 1 l volumetric flask and completed with distilled water until the mark

After measuring 50 ml of each sample were placed in Erlenmayer beakers, after than in each Erlenmayer beaker it was added 0,5 ml of 0,15 % methyl orange, 1 ml of NaOH 10 % and 20 ml of chloroform .(Figure 2).

They were stirred for 3 minutes, after 5 ml of HCl 2N was added over each mixture (Figure 3).

Figure 2. Mixtures created.

Figure 3. Mixtures after addition HCl 2N

The extinctions at the spectrophotometer were measured at 508 nm in the 1 cm vat against the reagent control (in our case being the distilled water). The extinction value of the sample was related to the standard curve obtaining the respective concentration in µg of cationic detergent in the sample.

Analysis of anionic detergents

Principle: anionic detergents with methylene blue form a compound of blue color, extractable in chloroform. The sensitivity of the reaction is 10 µg/ml. Aromatic amines can cause the intensity of the final color to decrease. [14]

Reagents: anionic detergent, sol. 1N sodium hydroxide, 1N sulfuric acid solution, chloroform, concentrated sulfuric acid and monosodium phosphate monohydrate.

***Materials*:** volumetric flasks, Erlenmayer glasses, technical balance, cylinder, funnel

Preparation of methylene blue reagent: an exact amount of 0.01g methylene blue dissolved in 10 ml of water, after that were added 25 ml of water, 3.4 ml of cc. sulfuric acid, 25 g of monosodium phosphate monohydrate and water to the 500 ml.

Working method: were prepared different concentrations from solution:

C1- weighed 0.02 g detergent, placed in a 1 l volumetric flask and supplemented with distilled water to the mark

C2- weighed 0.01 g detergent, placed in a 1 l volumetric flask and supplemented with distilled water to the mark

C3- weighed 0.03 g detergent, placed in a 1 l volumetric flask and filled in with distilled water to the mark

C4- unknown concentration, x.

Each sample was alkalized with sodium hydroxide (NaOH 1N) in the presence of the red Congo indicator until the pink-purplish turn (Figure 4.), after they faded with 1N sulfuric acid. The colourless solutions were treated with 10 ml of chloroform and 25 ml of methylene blue reagent. For quantitative isolation, the extraction operation in chloroform was repeated, initially with 10 ml, then with a further 5 ml CHCl3 (Figure 5.). Each sample was purified with 50 ml of 10 % monosodium phosphate solution monohydrate, which contained 1,3 ml H2SO4 cc.

The extinctions of the samples and standards to the spectrophotometer were measured at 589 nm in the 1 cm vat (figure 3.19)) relative to CHCl3. The extinction value of the sample was related to the standard curve, obtaining the respective concentration C in µg of anionic detergent in the sample.

Figure 4. Sample-solutions with anionic detergent(before H2SO4)

Figure 5. Samples after methylene ad.blue

RESULTS AND DISCUSSION

The absorbance readings were performed for the standard solutions and for the analysis sample from the cationic detergent at a wavelength of 508 nm. The results obtained in Figure 6 indicate that the optimal wavelength is 508 nm.

The following table (Table 1.) shows the absorbances of the standard solutions.

Based on the calibration curve, the sample concentration results is Cx= 0,00331.

Calculation:

*Mg cationic detergent/100 ml analyzed product=2*C/1000=*

$2*0,00331/1000=662*10^{-5}$

Figure 8 shows that the optimal wavelength for the analysis of anionic detergents is 589 nm.

Absorbance readings were taken for standard solutions and for analysis of anionic detergent at a wavelength of 598 nm.

Based on the calibration curve, figure 9., the concentration Cx = 0.011.

The following table (Table 2.) shows the absorbances of the standard solutions.

Calculation: The result it was expressed in anionic detergent:

mg detergent/ 100 ml = C/1000 = 0,011/1000= 11 10*$^{-4}$

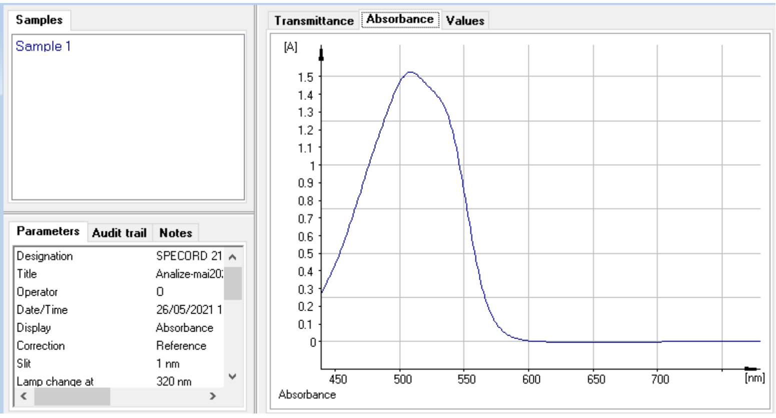

Designation	SPECORD 21
Title	Analize-mai20
Operator	0
Date/Time	26/05/2021 1
Display	Absorbance
Correction	Reference
Slit	1 nm
Lamp change at	320 nm

Figure 6. Absorption spectrum when analyzing cationic detergents

Table 1. Absorbents of standard solutions for cationic detergents

Concentraţii,	0,001	0,01	0,1	Cx
Absorbanţe	1,5241	1,5598	1,7192	1,5938

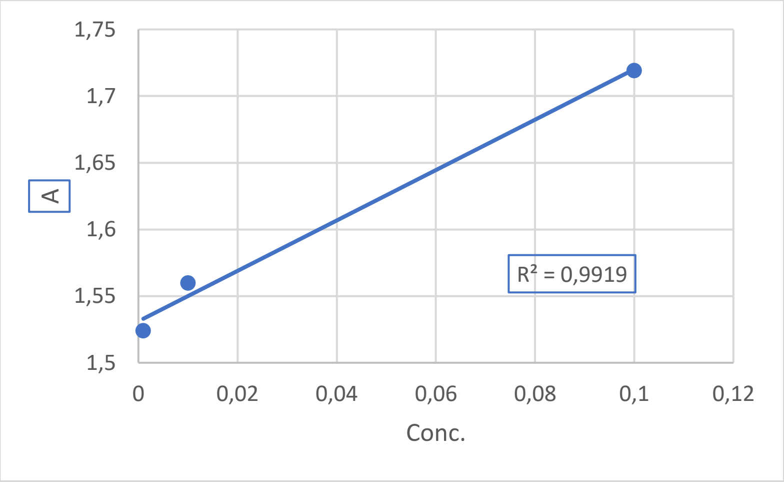

Figure 7. Calibration curve for the analysis of cationic detergents

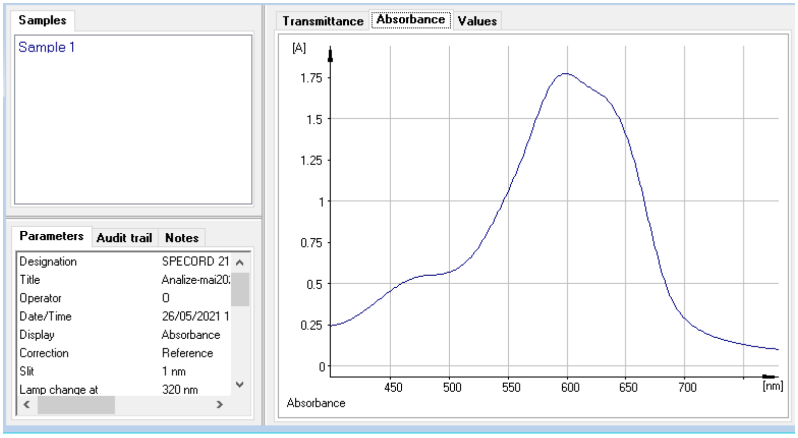

Designation SPECORD 21
Title Analize-mai20
Operator 0
Date/Time 26/05/2021 1
Display Absorbance
Correction Reference
Slit 1 nm
Lamp change at 320 nm

Figure 8. Absorption spectrum when analyzing anionic detergents

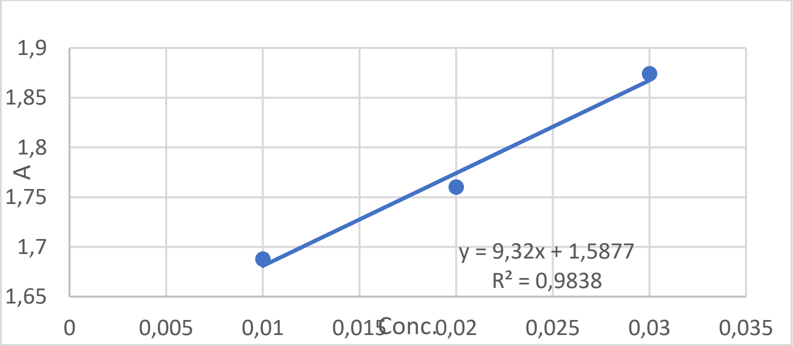

Figure 9. Calibration curve for the analysis of anionic detergents

Table 2. Absorbances of standard solutions

Concentraţii,	0,01		0,02	0,03	Cx
Absorbanţe	1,6878		1,7603	1,8742	1,6974

CONCLUSION

In order to analyze the content of anionic and cationic detergents from the point of view of some toxic substances, spectrophotometric determinations were made in this work. Thus, benzalkonium chloride, a cationic detergent in the water and an anionic detergent were analyzed.

Detergents used in various fields have attracted the attention of the scientific community due to environmental pollution, especially with surfactants, which are not effectively removed by wastewater treatment processes, but are not frequently monitored due to a lack of regulation. Therefore, the environmental impact of these compounds must be assessed on the basis of reliable data in different areas, including toxicity, biodegrabilityThe influence of the surface agents is multiple and complex, manifesting itself, especially, on the appearance and physico-chemical properties of water, fauna and flora. Biodegradability in the process of self-protection is of particular importance for environmental protection. The acute toxic effect of cationic surfactants on algae varies at concentrations of 0.03-11 mg/l.

REFERENCES

[1]- Radu A., Ioan C., Lambrache P., Angela L., Ion I., Petre C. (2004). Surfactanți, București, p.3-12

[2]- Scott M. J. and Jones M. N., 2000. The biodegradation of surfactants in the environment. // Biochimica et Biophysica Acta, vol. 1508, no. 1-2, p. 235–251.

[3]- Gheorghe Ştefania, Irina Lucaciu, Grumaz Rozalia, Stoica Cătălina.(2012). Acute toxicity assessment of several cationic and amphoteric surfactants on aquatic organisms. //*Journal of Environmental Protection and Ecology,* vol.13, no.2, p. 541-553.

[4]- Ivan G. Stefania,2012. Teza de doctorat, Bucuresti

[5]- Ivankovic T., Hrenovic J.,2010. Surfactants in the Environment. //Arh. Hig. Rada Toksicol,no. 61(1), p. 95-110

[6]-Rosen M.J., Kunjappu J.T.,2004. Surfactants and Interfacial Phenomena. Third edition. // New York, 455 p. 23. Sandu M., Spataru P., Mosanu E. 2009. Impact of surface active-substances on the natural waters self-purification. //Mater. Simpozion Internaţional „Mediul şi Industria - SIMI 2009", Bucureşti, p. 177.

[7]- Sandu M., Spataru P., Negru M., Mosanu E., Draguţan D., Goreacioc T. 25 –27 octombrie 2007. Dinamica procesului de nitrificare in prezenta substanţelor tensioactive cationice. //Mater. Simp. Internat. „Mediul şi Industria", Bucureşti,. p. 105.

[8]- Spătaru Petru, Sandu Maria, Tărîţă Anatol, Lupaşcu Tudor, etc. ,2011, Impactul substanţelor tensioactive asupra oxidării biochimice a ionilor amoniului în apele naturale. //Buletinul AŞM. Ştiinţele vieţii, nr. 2(314), p. 178-184.

[9]- 1981.The method for the determination of cationic surfactants with the disulphine blue method (DBAS). //Standards: T 73-280 and DIN 38 409 Teil 20 HMSO

[10]- Berger H. 7-8 April 1997, Environmentally compatible surfactants for the cosmetic industry, presented at the SCS Symposium.. //International Journal of Cosmetic Science, Bristol. no. 19, p. 227–237.

[11]- Berth P., Schwuger M.J. 1979, Chemical aspects of washing and cleaning. //Tenside Surfactants Detergents, nr. 16(4), p. 175-184.

[12]- Boiteux, J.P. 1984, Dosage colorimetrique d'agents de surface amphoteres et etude du compartement d'une alkyl amido betaine en milieu naturel. //La Revista italiana delle sostenze grasse. vol. LXI, p. 491-495.

[13]- Naşcu H., Jäntschi L. Hodişan T., Cimpoiu C., Câmpan G.(1999). Some Applications of Statistics in Analytical Chemistry, *Review Anal. Chem.*

(12pt)

INSTRUCTIONS FOR AUTHORS (TIMES 14 PT BOLD, CAPITAL LETTERS, CENTRED)

(12pt)

First name SURNAME[1], First name SURNAME[2] (12 pt bold)

[1]Affiliations and addresses (12 pt)

(12pt)

Abstract: *Abstract of 50-120 words (12 pt italic). It contains concise information about: objectives of the work, the results obtained, conclusions*

Key words: List 2-6 keywords. (l0 pt, italic).

(12pt)

INTRODUCTION (l2PT. CAPITAL, BOLD)

The paper has to be written in English. Each paper should be concise including text, figures and tables. Authors are kindly requested to submit in electronic format, Microsoft Word file form, 2003, 2007, 2010. The suggested structure of the main text: Introduction; Methods and Materials, Results and Discussions; Conclusions; References. (12pt)

INFORMATION (12 PT CAPITAL, BOLD)

Page layout:Use A4 format (210 x 297 mm), Margins: Top – 2,5cm, Bottom - 3 cm, Left- 4 cm and Right - 3 cm Paragraphs: alignment - justified, line spacing – 1,

Font style: Times New Roman.Text: l2pt.: regular, text in tables: 10 pt, 1 line space and centred, 2 columns, Equations: Equation editor, 12 pt, centred,References (12pt)

caption of tables and figures: 12 pt, italic

Tables, together with figures should be placed in their order of appearance in the text and numbered consecutively. Table captions containing the number of the table, and should be placed above the table. Tables should be clearly captioned and all symbols should be properly explained in either the table or its caption.

Figures (min. 300 dpi) can be in colour, but must also be clear enough for black and white reproduction. They should be centred and numbered consecutively and so referred to in the text. Each must be clearly captioned (after the Figure number) below the figure. Equations will be centred and numbered consecutively (right aligned).

All references would be cited in brakets [1*]

All papers cited should be listed under the **REFERENCES** (1 column), in order of appearance (Journal Article)

[1] Abbott, M. B., Petersen, M. M., and Skovgaard, O. (1978). On the numerical modelling of short waves in shallow water, Jnl Hydraulic Res; Vol 16 (3), pp. 23-44.

(Report)

[2] Carter, B., and Connell, C. (1980). Moa Point Wastewater Treatment Plant and Outfall Study, Report for the Wellington City Council, Wellington, pp. 31.

(Book)

[3] Grady, C.P.L., and Lim, H.(1980). Biological Wastewater Treatment Theory and Application, Marcel Dekker, New York, pp. 375.